NOVEL SENSOR FOR RAPID DETECTION OF BLOOD CELL TYPES-

MAGNETOSTRICTIVE MICROCANTILEVERS

Except where reference is made to the work of others, the work described in this thesis is my own or was done in collaboration with my advisory committee. This thesis does not include proprietary of classified information.

_____

Lisa Lorraine Orona

Certificate of Approval:

_____	_____
Aleksandr Simonian Assistant Professor Materials Engineering	Zhong Yang Cheng, Chair Associate Professor Materials Engineering
_____	_____
Jeffrey W. Fergus Associate Professor Materials Engineering	Stephen McFarland Acting Dean Graduate School

NOVEL SENSOR FOR RAPID DETECTION OF BLOOD CELL TYPES-

MAGNETOSTRICTIVE MICROCANTILEVERS

Lisa Lorraine Orona

A Thesis

Submitted to

the Graduate Faculty of

Auburn University

in the Partial fulfillment of the

Requirements for the

Degree of

Masters of Science

Auburn, Alabama
August 8, 2005

NOVEL SENSOR FOR RAPID DETECTION OF BLOOD CELL TYPES-

MAGNETOSTRICTIVE MICROCANTILEVERS

Lisa Lorraine Orona

_____

Author's Signature

_____

Date of Graduation

VITA

Lisa Lorraine Orona, daughter of Rudy and Maggie Orona, was born on November 4th, 1979, in Birmingham, Alabama. She attended Auburn University in Auburn, Alabama in September 1998 and graduated with honors with a Bachelor of Science in Materials Engineering in August 2003. After graduation, she continued her education by obtaining her masters degree in Materials engineering at Auburn University.

THESIS ABSTRACT

NOVEL SENSOR FOR RAPID DETECTION OF BLOOD CELL TYPES-

MAGNETOSTRICTIVE MICROCANTILEVERS

Lisa Lorraine Orona

Master of Science, August 8, 2005
(B.S., Auburn University, Auburn, 2003)

110 Typed Pages

Directed by Dr. ZhongYang Cheng

Microcantilevers have been around since the development of atomic force microscopy. The main attraction of cantilevers results from the fact that they can transduce many different signal domains into mechanical signals. Microcantilevers have different operational modes, but the one presented in this thesis is the dynamic microcantilever. Dynamic mode involves oscillation of the microcantilever at its resonance frequency. The main attraction of dynamic microcantilevers is that their resonance frequency is directly related to the mass attached to the microcantilever. Whenever mass is added to the surface of a microcantilever, a shift of resonance frequency will result. By monitoring the resonance frequency shift, the amount of mass added to the microcantilever can be determined. This type of detection can be applied

in different fields including food science, environmental monitoring, and medical industries. Bacteria detection that usually takes up to a couple of days for identification can be analyzed within minutes using sensors like microcantilevers. Recently, more publications are focusing on employing microcantilevers as biosensors to detect anything from *Salmonella* in food to *E-coli* in water. The objective of this thesis is to fabricate magnetostrictive microcantilevers and demonstrate the capabilities and advantages by using them to detect blood types. By observing the resonance frequency shift of the magnetostrictive microcantilevers, A and B blood types can be distinguished. Also presented in this thesis is the development of magnetostrictive thin films by electrochemical deposition. The thin film process allows numerous sensors to be fabricated with sizes ranging into the microns. These sensors can be made into microcantilevers. The magnetostrictive microcantilevers presented here can be driven and sensed wirelessly and also have a higher quality-value (Q-value) than other microcantilevers. By observing shifts in its resonance frequency due to blood cell loading, there seems to be some potential in being able to distinguish between certain blood types

ACKNOWLEDGEMENTS

The author would like to express her sincere thanks and gratitude to her major professor, Dr. ZhongYang Cheng, for his guidance, advice, and support during her graduate studies. She would also like to thank Dr. Jeffrey W. Fergus for his wonderful advice and guidance through her undergraduate and graduate degree. Thanks are also due to Dr. Aleksandr Simonian for his helpful discussions and insightful suggestions.

The author would also like thank Suiqiong Li for all her advice, suggestions, and help during my entire time performing research. Special thanks are giving to Charles Mithchell for all my formatting corrections. Appreciation is due to Dr. Zhimin Li, Vivek Krishnan, Sheetal Paliwal, Srinivas Sista, Shankar Ganesh ,Chad Callender and Courtney Guasti for all their help and suggestions. Sincere gratitude is given to Major Leamon K. Viveros for all his help throughout my research.

The author would also like to thank her parents and her family for their love and unconditional support throughout her college career.

Style manual or journal used: Auburn University Guide To Preparation And Submission Of Thesis And Dissertations

Computer Software used: Microsoft Word XP, Microsoft Excel

TABLE OF CONTENTS

LIST OF FIGURES

LIST OF TABLES

1. INTRODUCTION

1.1 Blood-Type Identification

Blood typing or blood grouping was started in the early 1900's when an Austrian scientist, Karl Landsteiner, became curious on why blood transfusions sometimes saved peoples lives while at other times caused death. By examining blood under a microscope, Karl Landsteiner discovered two different molecules present on the surface of certain blood samples. He named the molecules A and B. This is why our blood types are named A, B, AB, and O. If a blood sample contains only A molecules Landsteiner named this blood sample blood type A. Similarly, if a sample contained only B molecules it was named blood type B. If a blood sample contained both A and B molecules it was named blood type AB. If a sample did not contain A or B molecules then it was named blood type O. This discovery of four different blood types earned Landsteiner the Nobel Prize in 1930 [Franklin Institute 2005]. The reasoning for death in earlier day blood transfusions was that when two different blood types such as A and B are mixed together, the blood cells form clumps in the blood vessels, which can cause health problems and even death.

The molecules that Landsteiner discovered were antigens. Antigens are anything that causes the body to launch an immune response against that antigen through the production of antibodies [Dr. Smith medical library 2005]. Antigens are located on the surface of blood cells. Based on the presence or absence of the antigens, the blood type of

an individual can be determined. As stated above A antigens are present in A-type blood and AB-type blood, B Antigens are present in B-type blood and AB-type blood, and the absence of antigen A or antigen B is found in O-type blood. Figure 1.1 shows the difference between all the blood groups.

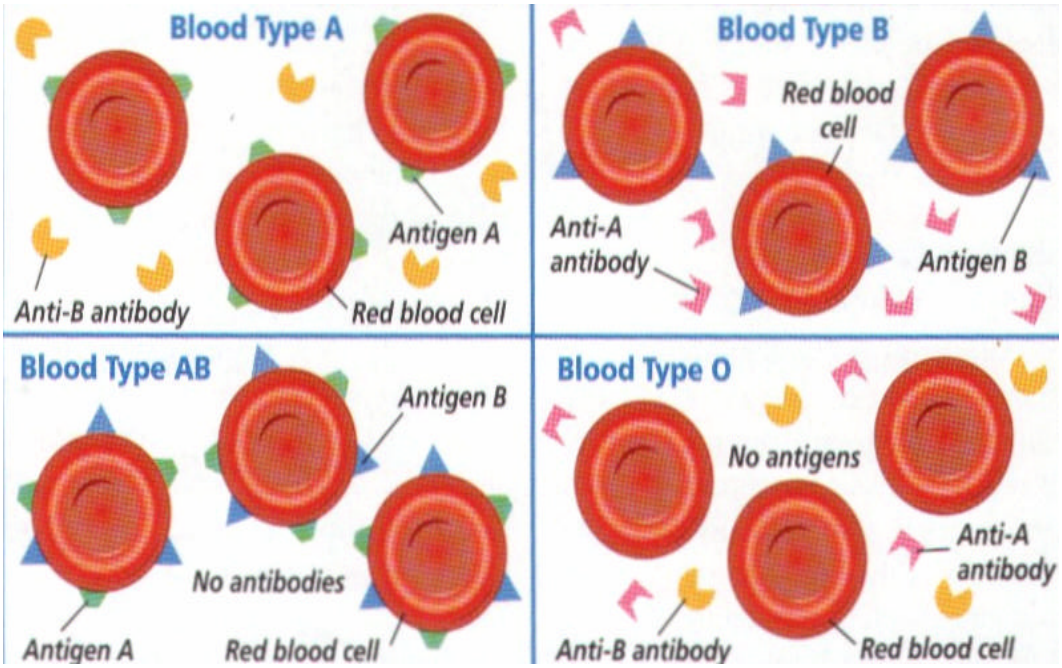

Figure 1.1: Difference between blood groups [Biology II 2005]

For example in blood type A, only A-antigens are present. Therefore, antibodies against B-antigens prevent producing type B or AB blood cells.

Current ways to determine a person's blood type are forward and reverse typing. In forward typing, a sample of blood is taken and mixed in one test tube with anti-A serum (serum that contains antibodies against type A blood) and mixed in another test tube with anti-B serum (serum that contains antibodies against type B blood). If the blood cells stick together in the test tube that contains anti-A serum then blood type A is present. In the test tube the antibodies attack and stick to the antigens, this results in the

formation of cell clumps. The same holds true for blood type B: anti-B antibodies stick to the B antigens. If the blood sticks together with both anti-A and anti-B serum, blood type AB is identified. Similarly if a sample of blood does not stick to either anti-A or anti-B serum then blood type O is present.

In reverse typing a person's own serum (the liquid portion of the blood without the cells) is mixed with known blood types A and B. For example, if B cells are mixed with a person's serum and clumps form, then type A blood is present. If A cells are mixed with a person's serum and clumps form, then type B blood is present. When a person has AB type blood, serum forms clumps with both A and B blood cells. When a person has O type blood, his/her serum doesn't clump with either A or B blood cells. Determining a particular blood type using forward and reverse typing is simply a process of elimination that usually takes about 15 to 30 minutes [Crestwood Medical Center 2005].

Manual blood typing is not the only means of determining blood types. Automation is another choice used by clinical laboratories. Two commercially available automated ABO typing are the Diamed ID-Sampler II and the ABS2000. Both methods use the same principle of forward and reverse grouping. These two machines look for clumping and no clumping of red blood cells. One study that evaluated the ABS2000 resulted in 5.63 hr/day less technician hands on time [LABMEDICE 2005]. Automation can result in high volume test results, less highly skill personal to run machines, and improved effectiveness of laboratory testing. With fewer technologist hands on time, automation can lead to fewer errors.

Enzyme-linked immunosorbent assays (ELISA) combined with a absorption-elution test have been proposed to determine ABO blood groups and proved to be effective [Watanabe 2002]. Biosensors have also been proposed for blood typing, SPR has also been tested to determine blood types [Kazuki 1999]. As will be demonstrated, microcantilevers have many advantages over current biosensors. In this thesis, a novel sensor - magnetostrictive microcantilevers for rapid detection of blood cell types is investigated. Also the technology to produce magnetostrictive materials for constructing magnetostrictive microcantilevers (MMCs) is studied.

1.2 Sensors and Biosensors

A sensor is defined as "a device that detects or measures a physical property, and records, indicates, or otherwise responds to it [Eggins 2002]". There are three types of sensors which include: physical sensors, chemical sensors, and biosensors. Physical sensors measure physical quantities like length, weight, temperature, pressure, and electricity, while a chemical sensor detects and measures a specific substance or set of chemicals [Eggins 2002]. A chemical sensor responds to a specific analyte (material to be determined quantitatively and qualitatively) through a chemical reaction. Biosensors are a subgroup of chemical sensors; the only difference is that they employ a biological sensing element.

A biosensor is composed of three parts: 1) a biological detection element, 2) transducer, and 3) a read-out system. See Figure 1.2.

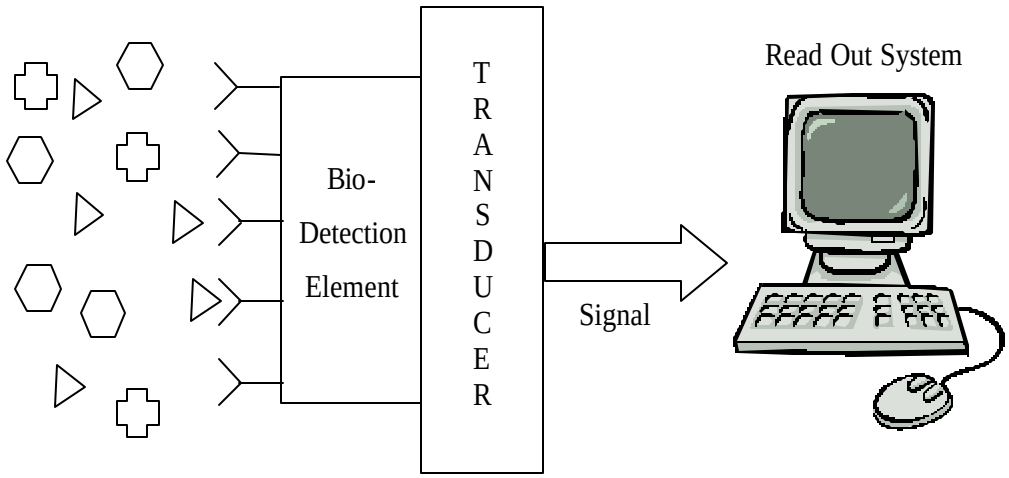

Figure 1.2: Schematic of Biosensor

The biological detector recognizes specific antigens/analytes. Analytes can be DNA/RNA, proteins, enzymes, whole cells, microorganisms, or antibodies. The transducer is a device that converts the observed change into a measurable signal. Some Biosensor transducers are classified as electrochemical, optical, piezo-electromechanical, or thermal. The read-out system filters, amplifies, displays, records, and transmits the measured signal [Raiteri 2002]. Biosensors can be classified by either detector type (such as immunosensors or enzymatic sensors), transduction principle (such as amperometric and piezo-electromechanical), or application (such as clinical sensors or environmental sensors).

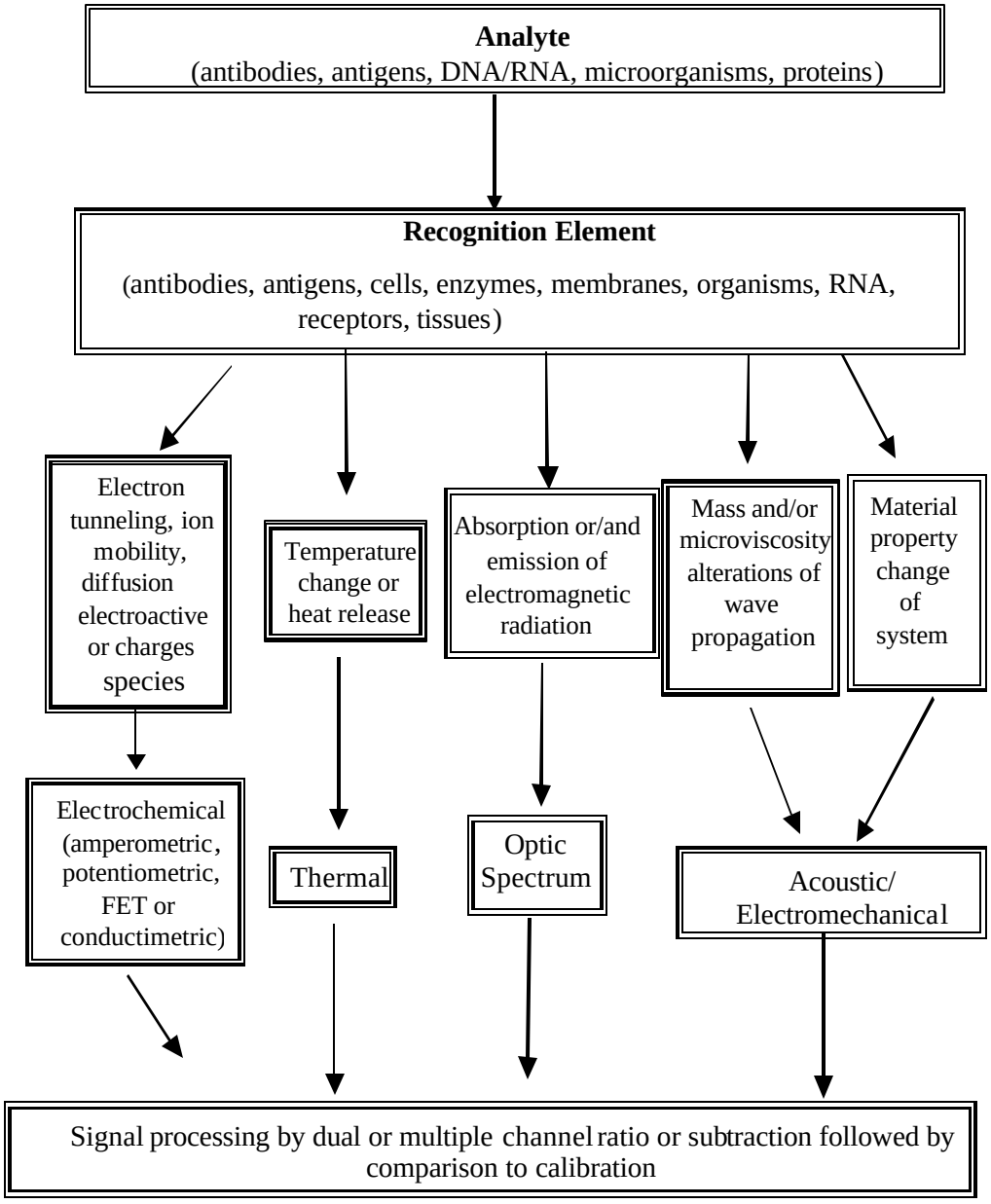

Figure 1.3: Biosensor Classification

Biosensors can be used in a number of fields including: clinical diagnostics, food analysis, environmental monitoring, military applications, pharmaceutical industry, and agriculture. For detecting pathogens in the food, traditional methods are time consuming. To specify different types of bacteria, colony counts can take up to 72 hours, which does not include the time to developme the colony that takes between 18 to 24 hours [Ivnitski 1999]. Bacteria identification can be processed within minutes using biosensors. Biosensors have numerous advantages including: low cost of fabrication, miniaturization, portability, rapid analysis time, high sensitivity, high specificity, on-the-spot analysis, real-time measurements, *in-situ* testing, and simple operation. The biosensors described in this chapter are the following: immunosensors; Surface Plasmon Resonance (SPR), Thickness Shear Mode (TSM) resonators, surface acoustic wave (SAW) devices, Flexural plate wave (FPW) devices, and microcantilevers. To understand how biosensors are useful and could eventually replace existing biological detection methods, enzyme-linked immunosorbent assay (ELISA) and polymerase chain reaction (PCR) are described first.

1.2.1 Conventional Biological Detection Methods

1.2.1a Polymerase Chain Reaction (PCR)

Polymerase chain reaction (PCR) or DNA replication has been used extensively since its introduction in 1985 [Kim 2002]. The power of PCR is phenomenal because infinitesimal amounts of DNA can be duplicated over billions of times. To perform PCR, DNA, primer, enzyme DNA polymerase, and four nucleotides are needed [Van 2001]. Three steps are involved in duplicating DNA (Figure 1.4). These steps include: denaturation, primer annealing, and primer extension. During denaturation the DNA

sample is heated and the double helix shape is separated into two single strands. Next in the primer annealing stage, the temperature is lowered and the primers bind to the single stranded DNA. In the last stage, at a higher temperature, the polymerase copies the rest of the DNA. After DNA replication, virus or pathogen detection from the DNA sample is performed by gel electrophoresis [Van 2001].

There are many areas where PCR can be used which include forensic, medical, environmental, and food sciences [Giakoumaki 2003]. PCR can detect disease pathogens like *Mycobacterium tuberculosis* in one to two days [Kim 2002]. *Salmonella* was detected by PCR in different forms like water, milk and blood samples [Ul-Hassan 2004]. The disadvantages of PCR stems from the fact that its extremely high sensitivity and low specificity can lead to false-positive results [Van 2001].

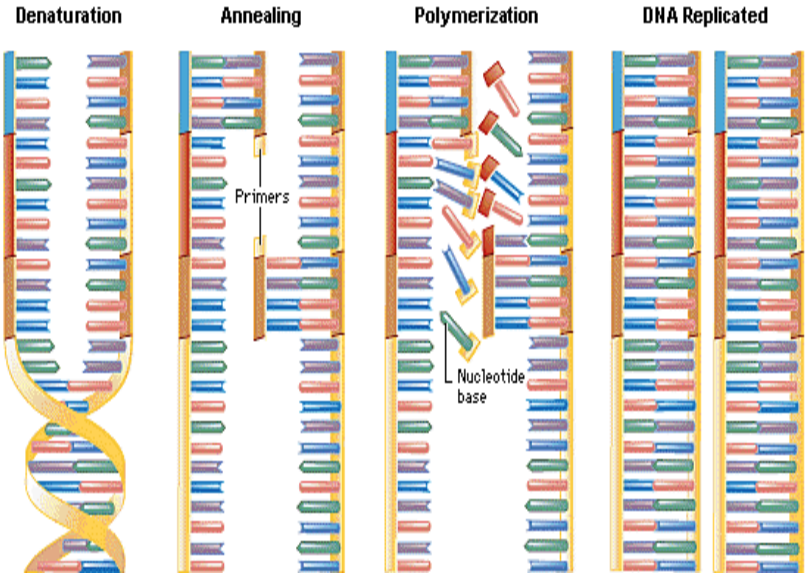

Figure 1.4: Three stages in duplicating DNA in polymerase chain reaction [MSN Encarta 2005]

1.2.1b Enzyme-Linked Immunosorbent Assay (ELISA)

Enzyme-linked immunosorbent assay (ELISA) techniques are being used today in a variety of fields including hospital facilities, environmental, clinical, agricultural, food and forensic laboratories [Piletsky 2001]. ELISA is a very simple process that includes the detection of antibodies or antigens. There are many different methods for detecting both antigens and the antibodies. In indirect ELISA for antibody detection, an antigen is immobilized either on a plastic bead or microtiter well. Then the sample to be tested is added to the bead or well. If the sample contains antibodies that are specific to the antigen, the antibody will attach to the antigen. Next, an enzyme labeled second antibody is added which is specific to the target antibody in the test sample. The second antibody will attach itself to the target antibody. Lastly a chromogenic substance is added. In presence of an enzyme labeled second antibody, the color will change [Kemeny 1988]. The amount of antibody in the sample can be measured by detecting the color change because the color change is proportional to the amount of antibody. Figure 1.5 is a schematic of indirect ELISA.

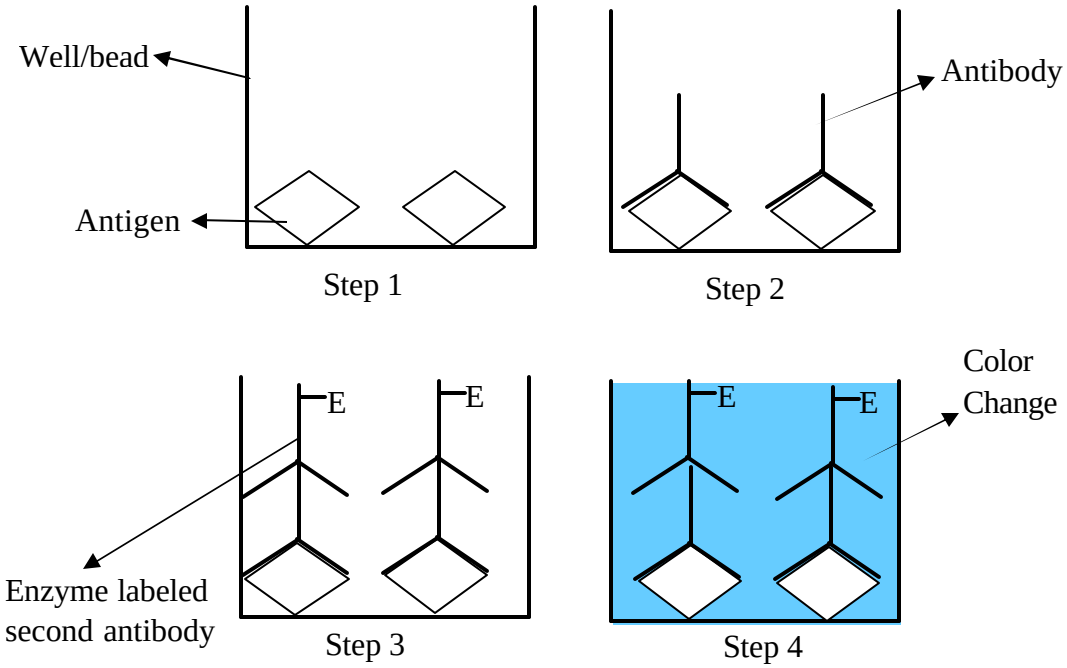

Figure 1.5: Schematic of indirect ELISA [Kemeny 1988]

There have been numerous papers written on ELISA capture. Some include analyzing the amount of pesticides in food and environmental samples [Nunes 1998], screening for penicillin plasma residues in cattle [Lee 2001], and detection of apoptotic cells and its application to rapid drug screening [Frankfurt 2001]. ELISA techniques have many advantages compared to classical analytical methods. These advantages include high sensitivity, rapid analysis time, cost-effectiveness, and simplicity [Nunes 1998].

1.2.2 Types of Biosensors

As mentioned early, a biosensor is comprised of three parts: the biological component, transducer, and the read-out system. Whenever the biological element on a biosensor is an antibody or antibody fragment, the sensor is called an immunosensor. Immunosensors detect the binding of an antigen to its specific antibody [Gizeli 1996].

Immunosensors can have optical transducers in which detection is based on changes in adsorption, fluorescence, luminescence, or refractive index due to light reflecting at the sensor surface [Luppa 2001]. They can have piezo-electromechanical transducers in which detection is based on mass changes or they can have electrochemical transducers in which detection is based on chemical potential [Ghindilia 1998].

Immunosensors have many advantages over immunoassays. The advantages include the following: sensor apparatus can be miniaturized, fewer steps are involved in assay procedure, sensitivity of assay is increased, time for analysis is decreased, procedure can be automated, and non-laboratory analysis [Ghindilia 1998].

Applications for immunosensors include microbiological analysis or environmental analysis. Even though there have been many papers on immunosensors, there are few commercial products.

1.2.2a Surface Plasmon Resonance (SPR)

Surface plasmon resonance (SPR) is used to detect target species based on optical property changes due to binding between target species and the molecular recognition layer. SPR is based on the principle of total internal reflection (TIR). When light impinges on a sample, which is made of two types of media with different refractive indices (one at a higher refractive media and one at a lower refractive media), at the interface it is partly reflected and partly refracted. When all the light is reflected from the higher refractive indices and the incidence angle is higher than a critical angle, total internal reflection is observed. In total internal reflection, not all the light is reflected by the surface. Actually the light partially enters the low refractive media to a distance of

one wavelength, which is called an evanescent wave [University of Waterloo 2005]. Since the interface between the two media is coated with a thin layer of gold, the evanescent wave excites molecules near the interface and couples with free oscillating electrons in the metal film [University of Waterloo 2005]. The binding of antigens to the antibodies that are on the surface of the sensor will result in a change in the effective refractive index of the outer layer. Figure 1.6 is a schematic of the phenomenon of surface plasmon resonance.

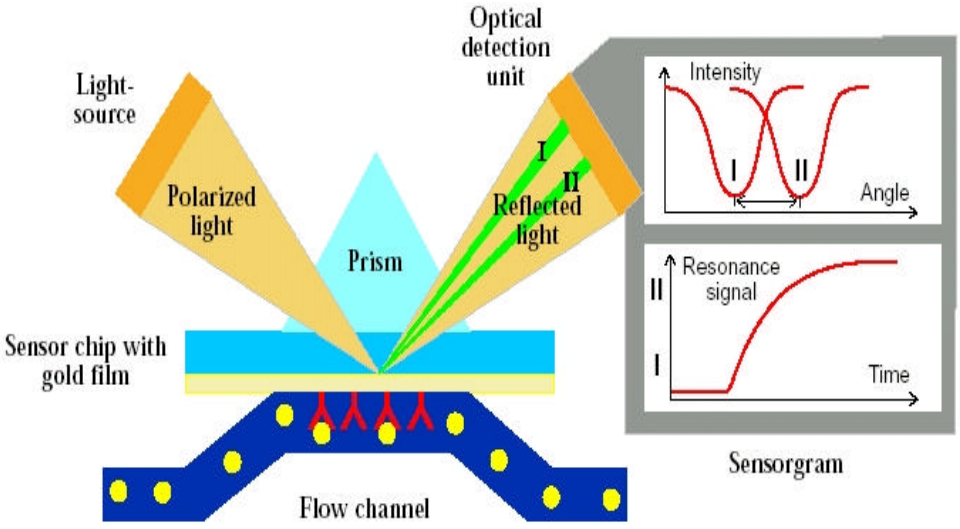

Figure 1.6: Schematic of Surface Plasmon Resonance [Biacore 2005]

SPR has a wide range of applications, such in the pharmaceutical industry for the purpose of drug discovery. It usually takes 12-15 years to develop the average drug which in turn can cost over $750 million dollars to produce [Myszka 2000]. SPR can lower the cost and increase drug throughput. SPR can also be used in detecting harmful food borne pathogens and chemical and biological warfare agents in military operations

[Naimushin 2005]. Studies have been performed using SPR to detect the foodborne pathogens such as *Salmonella* and *Listeria* [Koubova 2001]. SPR provides real-time measurements of analyte binding compared to end-point determinations as seen in ELISA. SPR requires no sample preparation for testing foodborne pathogens unlike polymerase chain reaction. PCR requires tedious sample preparation and the risk of cross-contamination DNA extracts with bacteria [Bokken 2003].

SPR offers simplie sample preparation and has a low risk of contaminating bacteria. SPR biosensors have also been used to detect chemical and biological warfare agents in an unmanned aerial vehicle [Naimushin 2005]. Even though there are many advantages to using SPR, it also has some disadvantages. These include keeping up with existing technologies on factors that include ease of use, low cost robustness, sensitivity, and stability [Homola 1999]. In order for SPR to be competitive it needs to improve on its detection limits, multi-channel performance, and development of advanced recognition elements [Homola 1999].

1.2.2b Thickness Shear Mode (TSM)

Acoustic wave devices have been in commercial use for over 60 years in numerous applications and the need for acoustic wave devices as sensors is continually growing [Drafts 2001]. The theory on how acoustic wave sensors work is contained within their name, acoustic waves. When acoustic waves propagate through or on a surface, any change in the acoustic propagation path, due to the interaction of the acoustic wave and the analyte, will result in changes in the acoustic wave properties. These wave properties can be measured mechanically or electrically. One advantage that acoustic

wave sensors have over other sensors is that they can monitor changes in two material properties, mechanical and electrical, as opposed to only a single material property [Andle 1994].

A piezoelectric material, like quartz, is used in acoustic wave sensors so that an acoustic wave can be formed. Once the acoustic wave is formed it can either travel through the piezoelectric substrate (bulk part) or on the surface of the substrate. After the wave has propagated through or across the entire substrate, the wave is converted back into an electric field for measurement. There are two main types of acoustic wave sensors that are categorized on how the acoustic wave travels. If the acoustic wave propagates through a substrate then it is known as a bulk acoustic wave sensor. If the acoustic wave travels along or near the surface of the piezoelectric substrate then it is known as a surface-generated acoustic wave device.

The most common and the oldest bulk device is the thickness shear mode resonator (TSM). As stated before, the name bulk stems from the fact that the acoustic wave travels through the substrate. The TSM resonator is also known as the quartz crystal microbalance (QCM). The TSM is composed of a thin circular disk of AT-cut quartz with two electrodes on both sides of the quartz. When a potential difference is applied across the electrodes, a strain on the crystal will be generated due to the piezoelectric effect. The voltage creates a resonance frequency in the crystal. When mass is applied on the TSM, change in the resonance frequency occurs. Therefore, TSM is a mass sensitive sensor. Based on the change in resonance frequency, the amount of analyte attached to the surface can be determined. The following figure is a schematic of the thickness shear-mode resonator device.

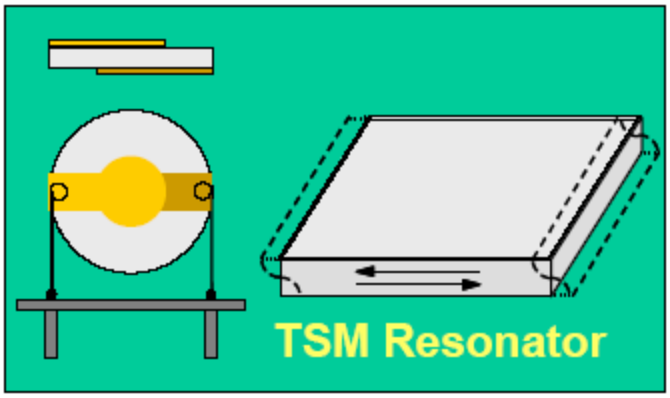

Figure 1.7: Schematic of TSM resonator [Cernosek 2005]

Advantages of using thickness shear mode resonators include their ability to withstand harsh environments and ability to be used in liquid [Drafts 2001]. Being able to use the TSM resonator in liquid opens many doors in using the TSM as a biosensor. Another advantage of the thickness shear mode resonator is its cost. Quartz is very inexpensive, so the fabrication of the sensors are cost efficient. TSM resonators also have a good quality factor, Q-value, in both liquid and air measurements. The quality factor (Q-value) determines the sharpness of the peak. It is related to the ratio of the resonance peak to the width at half the peak height. The higher the Q-value the more accurate it is to determine the resonance frequency. Since TSM resonators operate at a low frequency they have a low sensitivity. Biosensors that have a high sensitivity are able to detect small amounts of analytes. TSM resonators have the lowest sensitivity of all the acoustic wave devices [Drafts 2001].

1.2.2c Surface Acoustic Wave (SAW) Devices

The next group of acoustic wave devices is the surface-generated acoustic wave (SAW) device. The acoustic wave travels on the surface rather than in the bulk of the substrate. The phenomenon of the SAW was first mentioned in 1885 by Lord Rayleigh and has been used for electronic filters and signal processing applications since 1965 [Campbell 1989]. The SAW device has an interdigital transducer (IDT) that applies a radio frequency, which in turn produces mechanical stresses on the crystal. This produces a Raleigh-type surface acoustic wave. The wave travels along the surface until it is received by the other IDT, and then it is translated into an electrode voltage [Eggins 2002].

Like the TSM resonator, if some type of analyte is attached on the sensor surface then the transmission of the acoustic wave is affected. Instead of AT-cut quartz used in the TSM resonator, SAW devices use ST-cut quartz. The difference between AT and ST cut quartz is the orientation of the cut in the natural quartz crystal. Different quartz crystal cuts posses different properties. The SAW's small size, low cost, high sensitivity, and reliability have been used for chemical sensing applications. As stated earlier, TSM resonators have poor sensitivities as compared to SAW devices. Actually the mass sensitivity of the SAW device is 200 times greater than that of the TSM resonator because of the SAW's high operating frequency (1 GHz) in comparison with the TSM's operating frequency (10 MHz) [Galipeau 1997]. SAW devices are less expensive to fabricate than TSM resonators because SAW devices use standard microelectric fabrication that can be made in a wide range of designs. Figure 1.8 is a schematic of the surface acoustic wave device.

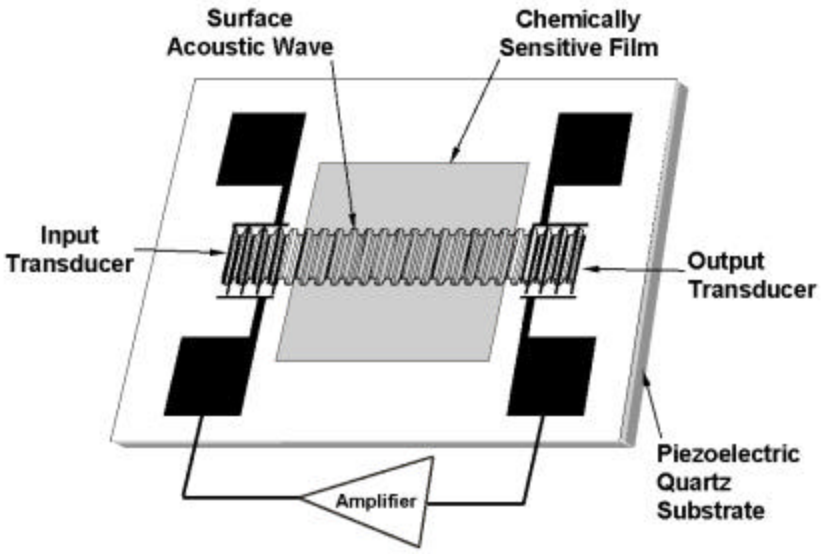

Figure 1.8: Schematic of SAW devive [Cernosek 2005]

SAW devices are good sensors for gas and air measurements, but poor sensors when it comes to liquid measurements. The reason for this major disadvantage is that when their acoustic waves get dampened in the liquid the specific signal from the sensors become distorted. Some applications of surface acoustic wave devices include gas detection, polymer characterization, dew point measurements, and measurements of surface energy [Galipeau 1997].

1.2.2d Flexural Plate Wave (FPW) Devices

The last acoustic wave device mentioned is the flexural plate wave device (FPW). Flexural plate devices have potential use in applications such as chemical, biological sensing, fluid pumping, and filtering [Weinberg 2000]. They can be used for vapor, liquid, or aqueous gel measurements.

Flexural plate wave devices are composed of plates, which have a thickness of about a fraction of an acoustic wavelength. The plate of some FPW devices is a composite that is composed of a silicon nitride layer, aluminum ground plane, and zinc oxide piezoelectric layer. The whole plate composite is on top of a silicon substrate [Hierlemann 2003]. Two interdigital transducers are fabricated on top of the composite plate. One IDT will generate the flexural wave and the other will receive the waves. When the IDT generates the flexural wave, the wave travels through the plate, which causes the entire plate to set into motion like ripples in a flag [Hierlemann 2003]. The entire plate composite undergoes deformation. The following is a schematic of the flexural plate wave device.

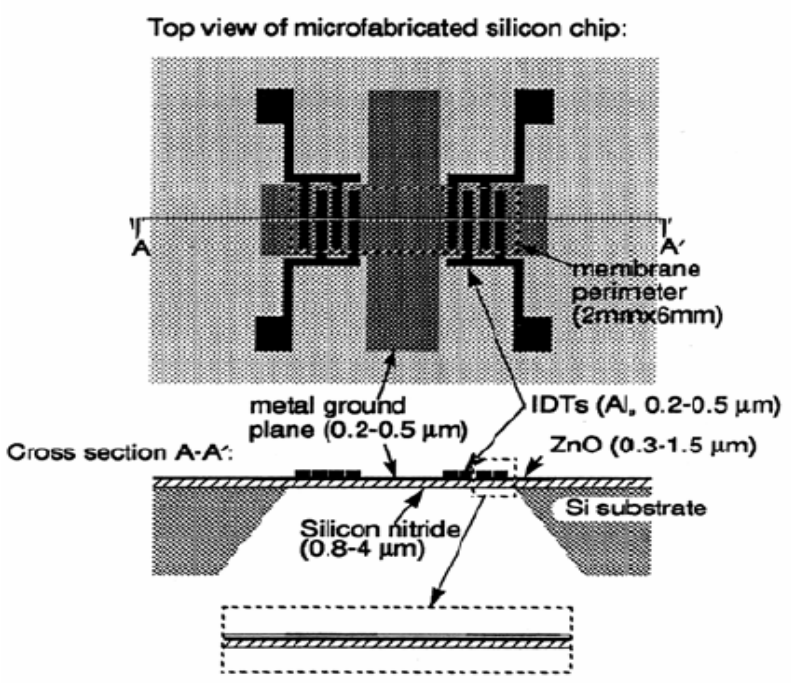

Figure 1.9: Schematic of FPW device [Cernosek 2005]

One of the major advantages of using FPW devices is that they have a higher sensitivity while operating at lower frequencies when compared with surface acoustic wave (SAW) devices [Shen 2002]. The following table is a breakdown of bulk devices, surface acoustic wave devices, and flexural wave plate devices in terms of mass sensitivity and operating frequencies.

Table 1.1: Comparison of Bulk, Surface, and Flexural Plate devices

Sensor	Theoretical Sensitivity	Device Description	Operating Frequency (MHz)	Calculated S_m value (cm^2/g)	Ref.
Bulk	-2/??	AT- cut quartz resonator	6	-14	[Wenzel 1990]
Surface	-K (s)/??	ST-cut SAW delay line	31 112	-42 -151	
Flexural Plate	-1/?d	ZnO/SiN flexural wave delay line	47 26	-450 -951	

S_m = mass sensitivities

? = density

s = Poisson ratio

d = thickness of the device material

? = wavelength

The mass sensitivity (S_m) for acoustic-wave oscillators is defined as the following:

$$S_m = \lim_{\Delta m \to 0} \frac{1}{f} \frac{\Delta f}{\Delta m} \qquad (1.1)$$

where ? m is the change of surface mass per unit area on the surface (g/cm^2) and ? f is the change in acoustic frequency (f) due to the mass load (? f)

1.2.2e Microcantilevers

Even though microcantilevers have been receiving recognition within the last few of years as biochemical and physical sensors, they have been present since the development of atomic force microscopy (AFM) in 1986 [Raiteri 2002]. In atomic force microscopy, the sensor consists of a cantilever, which is a long and thin microscopic beam fixed at one end with a support, and a sharp tip placed on the end of the free standing cantilever. AFMs are force sensors that are used to image the topography of a surface. Most commercially available cantilevers are made from silicon, silicon oxide, or silicon nitride. These cantilevers vary in shape and sensitivity. Cantilevers can transduce many different signal domains into mechanical signals. These signals can either be based on mass, temperature, heat, electromagnetic field and stress [Raiteri 2001]. They can be used in air, liquid, and harsh environments. Cantilever sensors work by specific analytes attaching onto the cantilever surface which results in a change in resonance frequency or stress-induced bending of the cantilever [Fagan 2000]. Today microcantilevers as opposed to macrocantilevers are more popular. Microcantilevers are preferred over macrocantilevers because they respond faster, cost less to fabricate, are more compact, and more importantly they have a higher sensitivity [Raiteri 2001].

The three operation modes that cantilevers work in are static, dynamic, or bimetallic heat. Static mode relies on cantilever deflection/bending due to surface stress changes on the cantilever that occur because of the analyte interaction [Battiston 2001].

In dynamic mode, the cantilever is oscillated at its resonance frequency. The resonance frequency changes with the mass load [Lang 2005]. In bimetallic heat mode, the cantilever is composed of two different types of materials with different thermal expansion coefficients. Changes in temperature or heat dissipated/adsorbed will cause the cantilever to bend [Raiteri 2001]. Figure 1.10 is a schematic of the cantilever sensor operating modes.

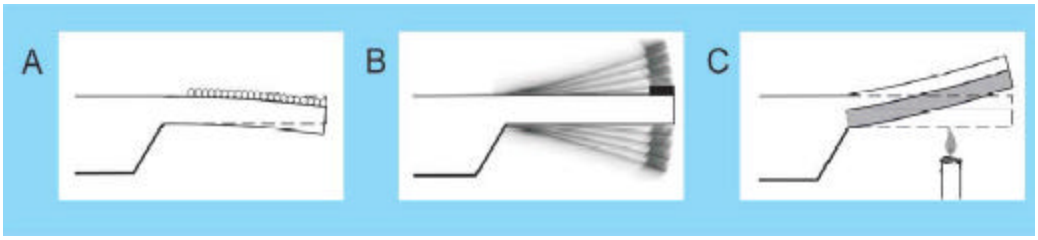

A) Static deflection modes; B) dynamic resonance mode; C) bimetallic heat mo

Figure 1.10: Operational Modes of Cantilevers [Lang 2005]

When cantilevers operate in static or dynamic modes, their detection of analyte absorption is based on the cantilever bending or change in resonance frequency. There are several deflection detection methods. These include optical lever, interferometry, capacitive sensor, and piezoresistive/piezoelectric cantilevers. In the optical lever method, a laser beam is focused at the freestanding part of the cantilever. When the analyte is absorbed, the cantilever bends and the reflected beam moves on a photodetector. Cantilever deflection is proportional to the distance traveled by the laser beam [Raiteri 2001]. A schematic of optical lever deflection detection is shown in the Figure 1.11.

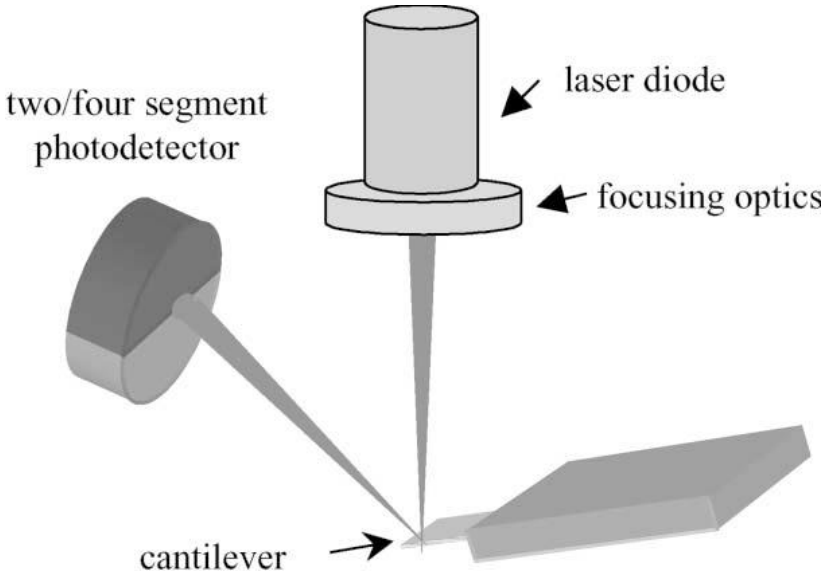

Figure 1.11: Optical lever deflection detection [Raiteri 2001]

Another type of optical detection is interferometry where the laser beam reflected from the cantilever is interfered with some type of reference laser beam. The two-laser beam interference detects the cantilever bending. This method allows direct and absolute measurement of the laser beam displacement. The deflection detection method of capacitive sensors operates by detecting changes in the capacitance of plane capacitors. This change in capacitance is caused by displacement in the cantilever. Piezoresisitive/piezoelectric cantilevers are primarily used in dynamic mode. Piezoresisitive/piezoelectric cantilevers have advantages over optical deflection detection techniques because there is no complicated laser alignment and any external optical components [Yang 2003]. The major disadvantage of optical deflection detection techniques is stress decay. When the analyte binds to the cantilever, the cantilever will bend temporarily because the induced binding stress decays with time [Yi 2003]. The

cantilever deflection can only be observed for the first 20 minutes because after this allotted time the induced stress will totally dissipate [Yi 2003]. In dynamic mode the binding induced stress in the microcantilever is not a factor, but only resonance frequency. The shift in resonance frequency is directly related to the change in mass. Analyte absorption can be detected long after it has been exposed to the target analyte.

Overall, microcantilevers have a number of advantages over other mass sensitive chemical sensors (e.g. surface acoustic wave (SAW), quartz crystal microbalance (QCM), and flexural plate wave devices (FPW)). Microcantilevers have a lower cost of fabrication and a smaller size that makes it portable for in-field applications [Zhou 2003]. Compared to SAW, QCM, and FPW, microcantilevers's sensitivity are two orders of magnitude greater [Fagan 2000]. Microcantilevers have been used frequently as chemical and physical sensors, but now recent publications report on their use for biosensing applications. Research on microcantilever-based biosensors has been reported for detecting certain protein makers of prostate cancer [Raiteri 2001]. These types of microcantilevers for prostate cancer detection are an alternative to ELISA techniques. Trying to detect food borne pathogens by monitoring resonance frequency shifts in a cantilever is being applied in research applications today. Cantilevers today are being used for a variety of applications which include: cantilever array systems (each cantilever is coated in order for it to be used as an artificial nose to identify vapors), gas-phase sensing for solvents using piezoelectric cantilevers, vapor and volatile vapor detection using static mode cantilevers and pH sensors [Lang 2005].

Microcantilevers that are made of non-piezoelectric materials like silicon are at a disadvantage compared to piezoelectric-based microcantilevers. Non-piezoelectric based

microcantilevers require either a high DC bias to operate or an optical system to determine its resonance frequency. Optical systems are complicated to operate, expensive, require large floor space, and are very difficult to be used in a liquid environment that is essential for biosensing applications.

Piezoelectric microcantilevers are attractive because the entire sensing system is located on the microcantilevers itself. There are two types of piezoelectric microcantilevers called the unimorph or bimorph. Unimorph microcantilevers are composed of a piezoelectric material layer and a substrate (non-piezoelectric material), while bimorph microcantilevers are made up of two piezoelectric layers. The later is a very complex structure, which makes it difficult to fabricate. Most research on microcantilevers have been based on unimorph structures. Although there is a great attraction for the high sensitivity in microcantilevers, there is a trade off in the quality value. The quality value or what some may call the Q-value is related to the ratio of the resonance peak to the width at half the peak height [Tamayo 2001]. The higher the Q-value, the higher the precision in determining resonance frequency of the microcantilever. Most piezoelectric based microcantilevers have a low Q-value. Additionally, when the microcantilevers are employed in liquid, the damping effect of the liquid media results in a significant deduction in Q-value. The Q-value for microcantilevers in air, range from a value of 30 -100 and then drop to a value less than 10 in liquid. There have been methods proposed to increase microcantilevers Q-values while in the liquid environment [Mertz 2001, Mehta 2001]. One proposed method was not to expose the entire cantilever to the liquid environment but only the tip of the cantilever [Yi 2003]. While another method was to expose the cantilever to the liquid

environment, remove and dry the cantilever, and then measure its resonance frequency shift [Ilic 2000, Ilic 2001]. Unfortunately neither these proposed methods have completely solved the problem of a low Q-value.

1.3 Magnetostriction

James Prescott Joule first discovered magnetostrictive materials in 1842 when he observed that a piece of iron changed its length in response to changes in magnetism [Etienne 1993]. Magnetostrictive materials undergo a shape change when an external magnetic field is applied, known as the Joule effect. The Joule effect occurs because the magnetic domains in the material align with the magnetic field (Figure 1.12).

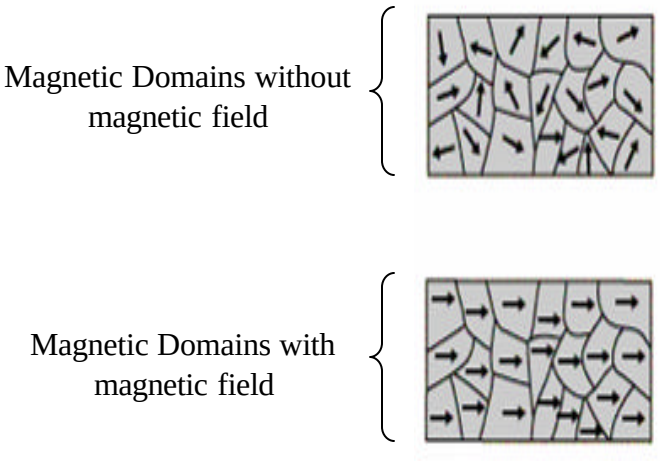

Figure 1.12: Magnetic Domains in presence of magnetic field [Ferromagnetism 2005]

Nearly all ferromagnetic materials exhibit a change in shape resulting from a change in magnetization. Magnetostriction will not degrade with time because it is an inherent material property. Earliest uses of magnetostrictive materials include telephone receivers,

torque-meters, and scanning sonar. In the past couple of decades, magnetostrictive alloys have been utilized to develop actuators, sensors, and dampers [Iowa State University 2003]. Giant magnetostrictive materials (GMM) have become commercially available with products like Terfernol-D and Metglass which came into existence in the mid to late 1980's[Iowa State Univeristy 2005]. By monitoring the shift in resonance frequency, magnetostrictive materials have been used as sensors to detect temperature, pH value, pressure, and viscosity [Grimes 1999, Qing 2000, Ruan 2003, Qing 2001, Puckett 2003].

2. OBJECTIVES OF RESEARCH

Magnetostrictive microcantilevers can be employed as a biosensor for different applications. Mass added on the surface can be detected by easily observing a shift in resonance frequency. The detected mass can range from bacteria, chemical warfare agents, and perhaps blood cells. The objective of this thesis was to fabricate magnetostrictive microcantilevers that could detect certain blood types mainly blood type A and blood type B. By observing the resonance frequency shift of the magnetostrictive microcantilevers, the two types of blood could be distinguished. The microfabrication technique of microcantilevers is explored by depositing a magnetostrictive thin film onto substrates and using this microfabrication process to pattern it into designed shapes and sizes.

3. PRINCIPLES OF MAGNETOSTRICTIVE MICROCANTILEVERS (MMCs)

3.1: Design

Microcantilevers are receiving much attention because they exhibit high-mass sensitivity (single cell detection), easy integration, and are compact in size. Most microcantilever research has focused their attention on either silicon-based or piezoelectric-based microcantilevers. Even though they exhibit the advantages just mentioned, they are faced with challenges. These challenges include low Q-values and ability to work in a liquid environment. Not being able to work in liquid environment limits the applications where these microcantilevers can be used.

Presented in this thesis is a new type of microcantilever- magnetostrictive-based microcantilevers. These types of microcantilevers offer the same advantages as other microcantilevers do and more. They are able to work in a liquid environment while obtaining a high Q-value. It has been found experimentally that Q-value of magnetostrictive microcantilevers can reach more than 250, which is much higher than other microcantilevers. Magnetostrictive microcantilevers are also easy to actuate, sense, and fabricate. Piezo-based microcantilevers are easier to actuate and sense compared to silicon-based cantilevers. This is because piezo-based cantilevers do not have to have an external optical system to detect the resonance frequency. On the other hand, piezo-based

cantilevers have a very complicated structure. They are composed of electrodes that are used for actuating and sensing. A voltage is applied to the electrodes and the converse piezoelectric effect causes the cantilever to vibrate [Yi 2001].These vibrations give rise to large piezoelectric voltages detected at the sensing electrodes by the direct piezoelectric effect [Yi 2001]. Also, if they are to be used in a conductive media, they need insulation. Figure 3.1 is a schematic of the cross-section of silicon-based, piezoelectric-based, and magnetostrictive-based microcantilevers.

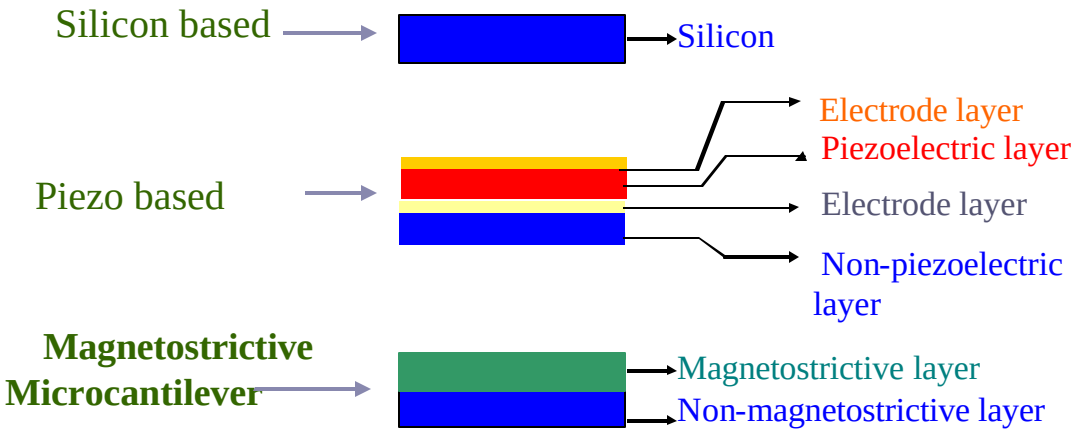

Figure 3.1: Cross-section of different cantilevers

3.2 Operation Principle of Magnetostrictive Microcantilevers

The operation principle of magnetostrictive microcantilevers is similar to acoustic wave mass devices. An increase in mass load on the sensor surface results in a shift in resonance frequency. The theory on resonant frequency generation can be explained as follows. Whenever an external magnetic field is applied, the dimensions of the magnetostrictive material changes along the applied magnetic field. Due to dimension

changes in the magnetostrictive material, the magnetic flux is irradiated because of the inverse Joule effect. Therefore, the magnetostrictive material converts magnetic energy into elastic energy. This energy conversion reaches its maximum when the frequency of driving magnetic field equals the nature resonant frequency of the magnetostrictive sensor. At this point the magnetostrictive sensor undergoes magnetoelastic resonance. The phase of magnetic flux generated by the magnetostrictive sensor is detected by the pick-up coil. The resonance frequency is the biggest phase of the magnetic flux. Figure 3.2 is an illustration of the resonance frequency detection for magnetostrictive microcantilevers.

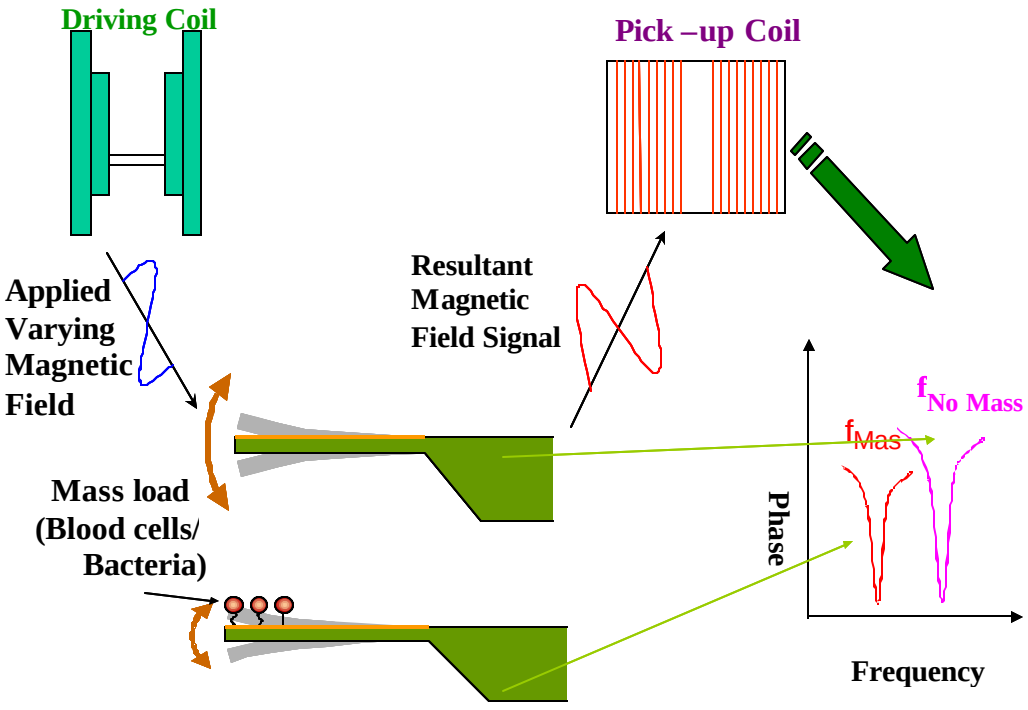

Figure 3.2: Resonance Frequency Detection

It is known that the theoretical flexural resonance frequency of a cantilever clamped at one end is [Ziegler 2004]:

$$f_n = \frac{l_n^2}{2p\sqrt{12}} \frac{t}{L^2} \sqrt{\frac{E}{r(1-n^2)}} \qquad (n=0,1,2,\ldots.) \qquad (3.1)$$

$?_n^2$ = dimensionless nth-mode eigenvalue ($?_0$ = 1.875)
t = thickness of cantilever
E = Effective Young's modulus
? = density
L = length of cantilever
? = Poisson Ration

From equation (3.1) it can be seen that the theoretical flexural resonance frequency is linearly dependent on its thickness and $1/L^2$ [Yi 2003].

In this thesis the magnetostrictive material, Metglas™, was polished to ~20µm, and the thickness of the copper sputtered on the magnetostrictive material was estimated at ~10µm. When calculating the theoretical resonance frequency, the thickness was estimated at ~30µm. The density of the commercial magnetostrictive material Metglas™ is 7.9 g/cm^3, and the density of copper is 8.9 g/cm^3. The effective density of the Metglas™/copper film is 8.23g/cm^3. Bulk copper has a Young's modulus of 130 GPa and the reported Young's modulus of sputtered copper film is 110 GPa [Read 1998]. For theoretical resonance frequency calculations, the Young's modulus was 110 GPa for both the Metglas™/copper film. Table 3.1 lists the known variables for the theoretical resonance frequency equation.

Table 3.1: Known Variables

Variables	Metglas™	Copper Film	Metglas™/Cu film
Density, ?	7.9 g/cm^3	8.9 g/cm^3	8.23 g/cm^3
Young's Modulus, E	100 GPa	110 GPa	110 GPa
Thickness, t	~20 μm	~10 μm	~30 μm
Poisson Ratio, ?	0.5	0.36	0.5

The mass sensitivity (S_m) of a cantilever is defined as the change in frequency divided by the mass load. It can be experimentally calculated by the following equation [Yi 2003]:

$$S_m = \frac{change\ in\ frequency}{mass\ load} = -\frac{\Delta f}{\Delta m} \tag{3.2}$$

Calculating the mass sensitivity theoretically depends on how the mass is loaded onto the cantilever surface. If the mass is loaded at the tip of the cantilever the mass sensitivity (S_m) is known as [Yi 2002]:

$$\left.\begin{aligned} S_m &= \frac{\Delta f_n}{\Delta m} \cong \frac{1}{2}\frac{f_n}{M_e} \\ EffectiveMass(M_e) &= 0.236Lwtr \\ S_m &= K_1 \frac{l_n^{\,2}}{L^3 w} \end{aligned}\right\} \tag{3.3}$$

$$K_1 = \frac{1}{0.944p\sqrt{12}}\sqrt{\frac{E}{r^3\left(1-u^2\right)}} \tag{3.4}$$

As can be seen from equation (3.3) and (3.4) the mass sensitivity is fundamentally depended on the material properties of the cantilever. It can be seen from equation (3.3) that the mass sensitivity increases with decreasing cantilever size [Yi 2003].

If the mass load is uniformly distributed on the cantilever surface, the mass sensitivity is known as [Yi 2002]:

$$\left.\begin{aligned} S_m &= \frac{\Delta f_n}{\Delta m} \cong \frac{1}{2}\frac{f_n}{M} \\ Mass(M) &= Lwtr \\ S_m &= K_2 \frac{l_n^{\,2}}{L^3 w} \end{aligned}\right\} \qquad (3.5)$$

$$K_2 = \frac{1}{4p\sqrt{12}}\sqrt{\frac{E}{r^3\left(1-u^2\right)}} \qquad (3.6)$$

K_1 represents the spring constant when the mass is loaded at the tip and K_2 represents the spring constant when the mass is loaded uniformly.

Figure 3.3 shows the relationship between mass sensitivities and varying cantilever lengths. The width of the cantilever is assumed to be 1/10 of the cantilevers length.

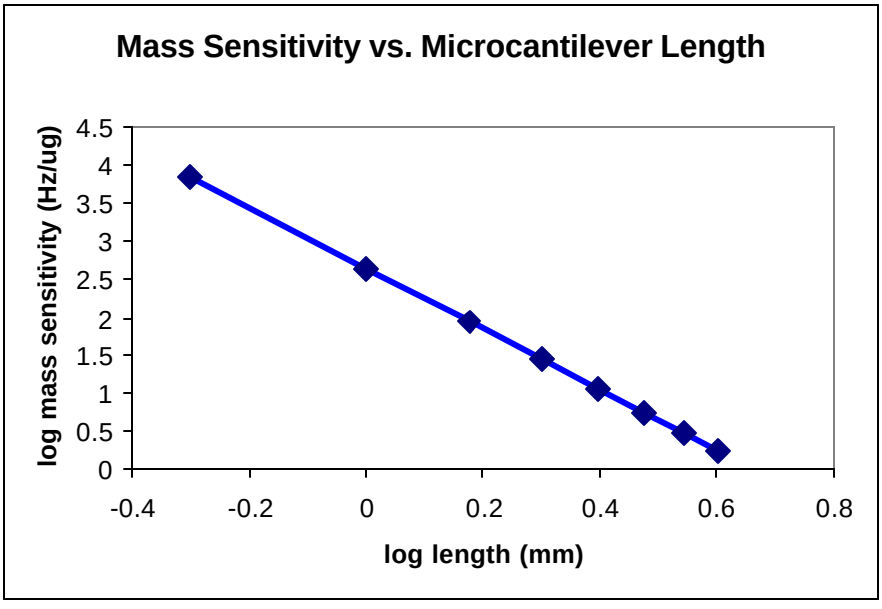

Figure 3.3: Relationship between mass sensitivity and microcantilever length

As can be seen from Figure 3.3, as the cantilevers length increased the mass sensitivity decreases. Figures 3.4 and 3.5 show the relationship between resonance frequency and cantilever length.

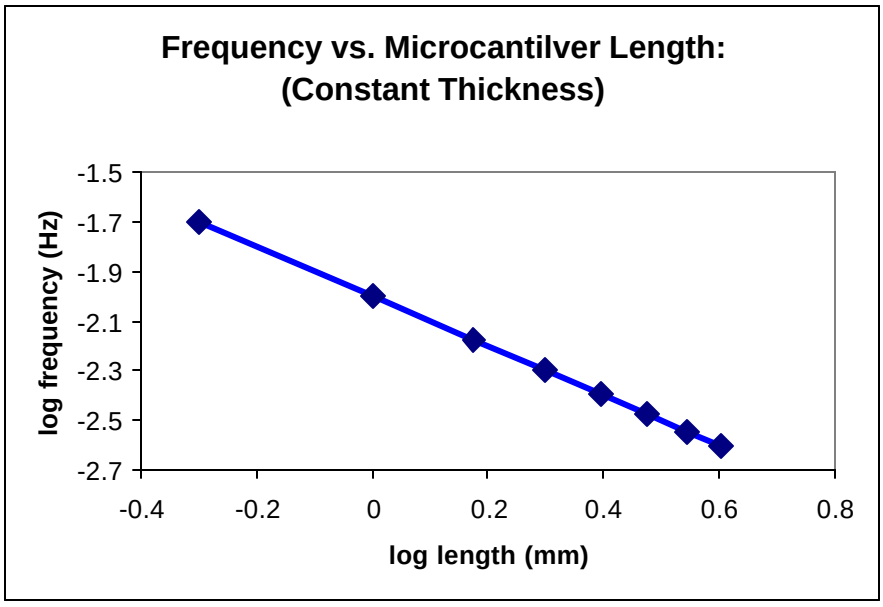

Figure 3.4: Relationship between resonance frequency and cantilever length

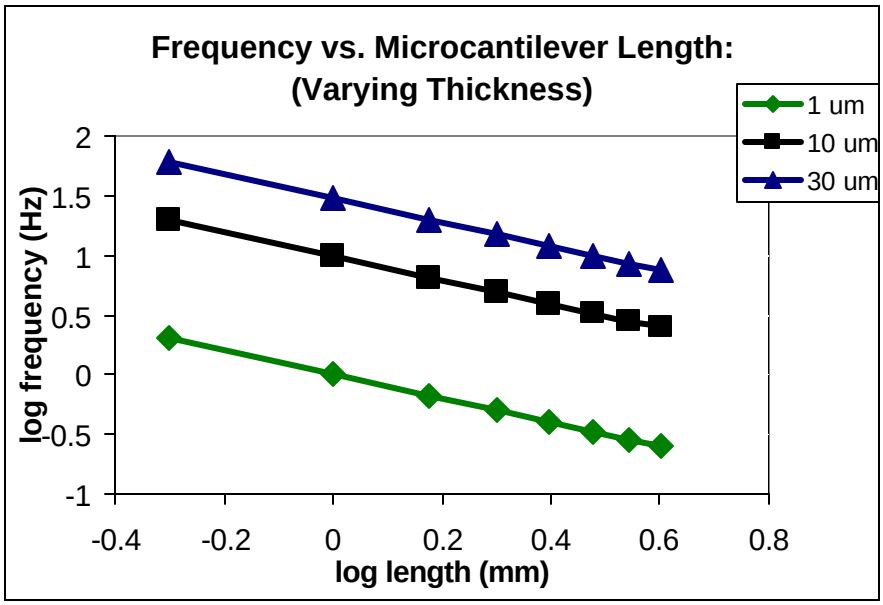

Figure 3.5: Relationship between resonance frequency and cantilever length

The thickness in Figure 3.4 is assumed to be 1% of the cantilevers length. As can be seen from Figure 3.4 as the cantilevers length decreases, the resonance frequency increases. The thickness is fixed in Figure 3.5. In Figure 3.5 resonance frequency also depends on the thickness of the cantilever. As the thickness increases the resonance frequency increases.

3.3 Resonance Frequency Determination

In this study, the measurement set-up includes a magnetic field generation (driving coil) and a signal pick-up system (pick-up coil). A custom designed Helmholtz coil generated the magnetic field. A homemade pick-up coil served as the pick-up system. The set-up for resonance frequency measurement is shown on Figure 4.2. The purpose of the pick-up coil was to collect the magnetic signal from the magnetostrictive

microcantilever. This signal was measured using a lock-in amplifier (SRS830, Standard research systems, Sunnyvale, CA). The lock-in amplifier puts out two signals: amplitude and the phase of the magnetic signal. The amplitude signal represented the oscillating amplitude of the cantilever, while the phase signal represented the phase difference between the AC driving field and the signal. In this research, the phase signal was used to determine the resonance behavior. The phase signal is a better indicator because it is independent of the amplitude of the signal. Figure 3.6 is a typical cure of the phase signal. The curve on the right represents the phase signal when no mass is added to the sensor, and the curve on the left represents the phase signal after mass is added to the sensor.

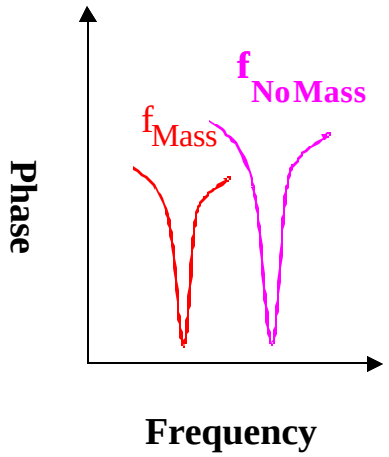

Figure 3.6: Schematic of phase signal verses frequency graph

The phase of the cantilever should decrease a little when mass is added to the sensor because the vibration of the cantilever is not as strong as it was when no mass was on the surface. The phase of vibration and the phase signal should be the same. The cantilever is

taken out of the pick-up coil and placed back in five different times for resonance frequency measurements. Therefore, the phase signal may not be the same as previous measurements because the cantilever may be placed at a slightly different location. To ensure the experimental resonance frequency was accurate, all the data was fitted using software. Peak fitting is one way to reduce noise and quantify peaks. After each resonance frequency was measured, the data was put into peak fitting software. The software uses a Gaussian response function. To determine the peak type, Gaussian amplitude spectroscopy function and a linear background were used and shown by Equation (3.7) is the Gaussian amplitude equation used in the peak fitting data software.

$$y = a_0 \exp\left[-\frac{1}{2}\left(\frac{x - a_1}{a_2}\right)^2\right] + (A + Bx) \qquad (3.7)$$

a_0 = Amplitude
a_1 = Center
a_2 = Width (std. dev)
(A+ Bx) = background, A and B are constant

Table 3.2 lists the frequency based on fitting data using Gaussian function over different frequency ranges and baselines.

Table 3.2: Fitted Frequency Data

Frequency Range (Hz)	Baseline	Frequency, f_0 (Hz)
1453-1467	Linear	1459.9
	Constant	1459.7
1419-1491	Linear	1459.5
	Constant	1459.7
1411-1586	Linear	1459.6
	Constant	1459.7
1354-1995	Linear	1459.5
	Constant	1459.7
Average	Linear	1459.6±0.32
	Constant	1459.7±0

3.4 MMCs vs. Current Microcantilevers

The work in this thesis uses cantilevers that operate in dynamic mode. These sensors can detect analyte absorption by observing a change in resonance frequency. The change in resonance frequency is directly related to mass absorption. As discussed above, most cantilevers are either silicon based or piezoelectric/piezoresistive based. Both have their advantages and disadvantages. Silicon based cantilevers are driven mechanically and their transducers are optical based. The main disadvantages of their optical system are associated with their bulkiness, the tedious alignment, and calibration of the laser. Some advantages of silicon based cantilevers are their easy fabrication, high Q-value, and high sensitivity. Piezoelectric/piezoresistive based cantilevers are driven electrically and

their transducer is an electric chip that is on the cantilever. Piezo-based cantilevers disadvantages include low Q-values, complicated sensor fabrication, and low sensitivity. Trade-offs exists between both the silicon-based and piezo-based cantilevers. The one major disadvantage that both cantilevers posses is when operated in a liquid environment they have a lower sensitivity. Liquid operation is a crucial aspect for biosensor application. For example, when detecting foodborne pathogens like *Listeria,* found in dairy products like milk or cheese, being able to produce real-time measurements in liquid is important. Also when detecting *E-coli* contamination in lakes or rivers, it is imperative that sensors work in water. The magnetostrictive-based microcantilevers are based on magnetostriction rather than piezoresistivity and therefore can be driven and sensed wirelessly. Their transduction element is magnetic so therefore no wires are need for a connection. Table 3.3 is a breakdown of the three types of microcantilevers just discussed.

Table 3.3: Comparison of Cantilevers

Characteristics	Silicon-Based	Piezo-Based	MMCs
Actuation	Mechanical	Electrical	Magnetic
Transduction	Optical (separated bulk system)	Electrical (on-board circuit)	Magnetic (wireless no connection)
Operate in Air	Yes	Yes	Yes
Operates in Liquid	Very Difficult	Very Difficult	Works Well
Q-value	High	Low	Very High
Structure	Very Simple	Complicated	Simple
Fabrication	Easy	Difficult	Easy
Overall Sensitivity	High	Low	High

The table demonstrates that magnetostrictive microcantilevers have advantages over both the silicon based and piezo- based sensors. The principle advantage of the magnetostrictive microcantilever is that it's operated by a magnetic field. It is driven and sensed wirelessly due to its magnetic and magnetostrictive nature.

The second part of this thesis was to produce thin films by electrochemical deposition. Once the magnetostrictive material was deposited onto a substrate, lithography was used to fabricate sensors into their designated shapes. This is a critical step to fabricating microcantilevers with different sizes.

4. EXPERIMENTAL

This section describes the fabrication and testing of magnetostrictive microcantilevers (MMCs) and also the fabrication of magnetostrictive thin films. The results obtained from the magnetostrictive microcantilevers (MMCs) and the thin film project will be discussed in the results and discussion section.

4.1 Synthesis and Fabrication of Magnetostrictive Microcantilevers (MMCs*)*

A magnetostrictive-base microcantilever (MMCs) was constructed with a commercial magnetostriction alloy, Metglas™ 2826MB ribbon with a thickness of 30µm from Honeywell (Morristown, NJ). The properties of the ribbon are shown in table 4.1.

Table 4.1: Properties of Metglas™ 2826

Composition	FeNiMoB (exact composition unknown)
Young's Modulus	100-110 GPa
Density	7.9 x10^3 kg/m^3
Poisson Ratio	0.50

The ribbon was first polished down to 20µm by using 2000# polish paper. After polishing, the ribbon was cleaned with acetone to remove any excess debris. Next a thin layer of chromium (Cr) (~100 nm thick) was deposited onto the strips using a magnetron RF sputtering technique. Then a thin layer of copper (Cu) was deposited (~ 10µm) onto the chromium layer using the magnetron DC sputtering technique. The chromium layer acted as an adhesion layer to the magnetostrictive material. Therefore the chromium/copper formed a bilayer structure. The Metglas™/copper ribbon was cut into strips with lengths ranging from 2.5 to 3mm and widths about 1mm. To form a cantilever each of these stripes were clamped at one end with a PMMA plastic holder. A layer of chromium and gold were deposited onto both sides of the cantilever using a sputtering technique. The chromium thickness was 100nm, while the gold thickness was 400nm. Gold was deposited on the cantilever because it protects against corrosion and provides a favorable binding site for antibodies and proteins. Once this was completed the cantilever was ready to be tested. Figure 4.1 shows a summary of the synthesis and fabrication of the microcantilevers. The set-up for resonance frequency measurement in the laboratory is shown in Figure 4.2. Figures 4.3 and 4.4 are pictures of the types of magnetostrictive cantilevers and the PMMA polymer crucibles used in experiments.

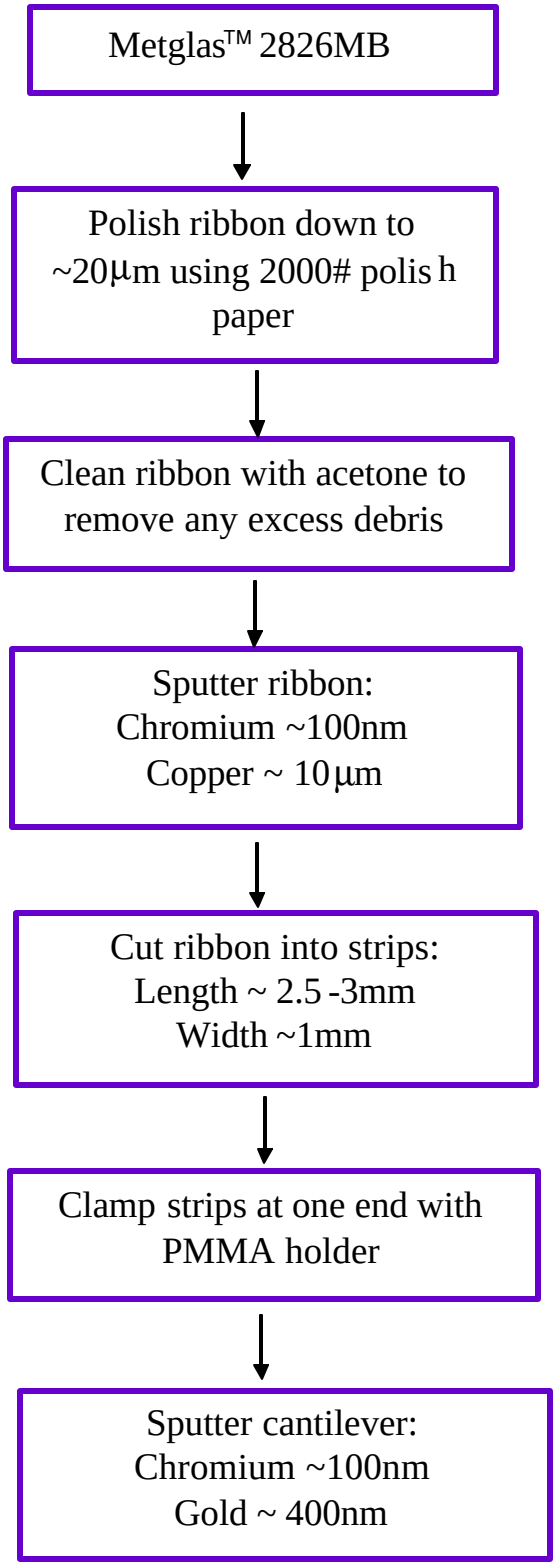

Figure 4.1: Steps in fabricating MMCs

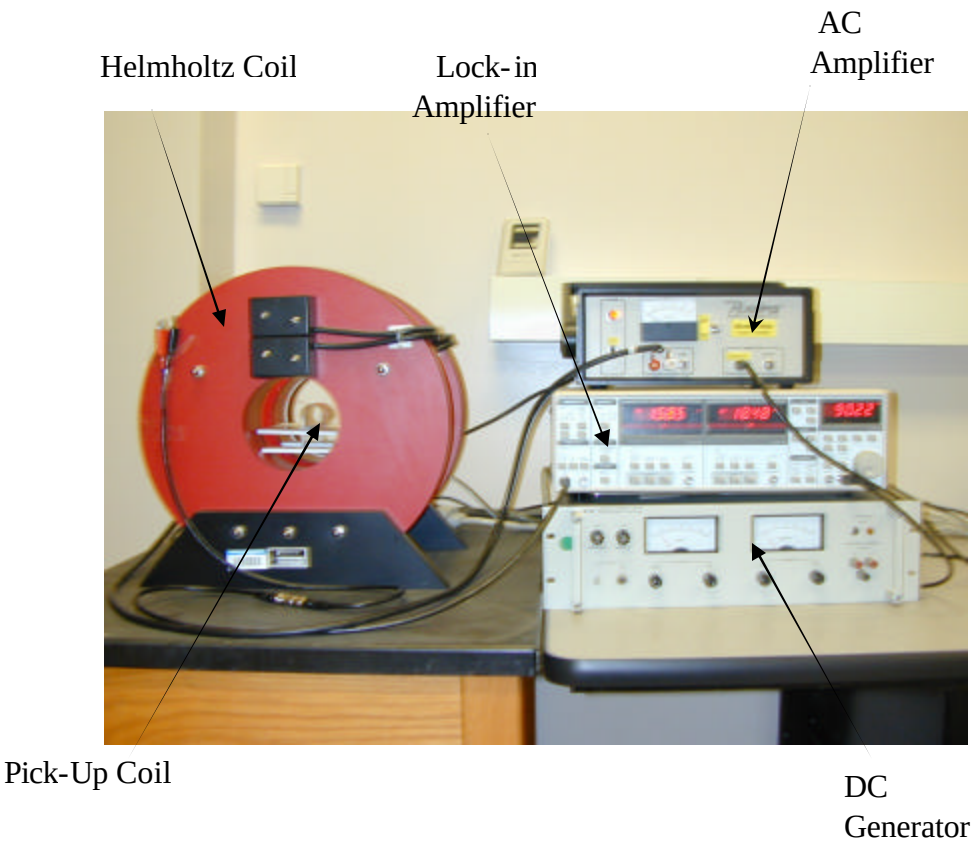

Figure 4.2: Measurement set-up in laboratory

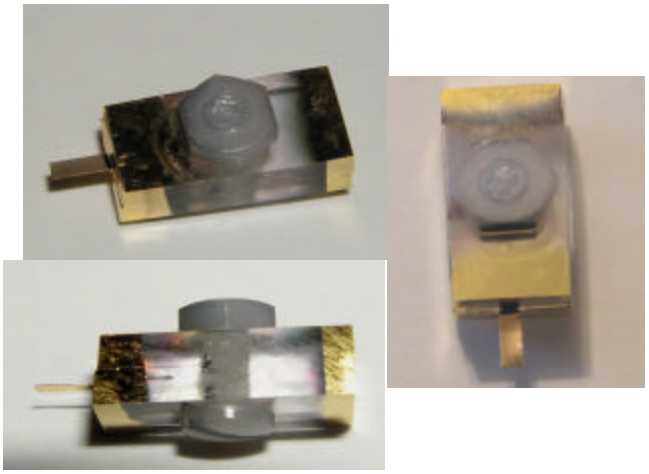

Figure 4.3: Front, side, and top view of gold coated cantilever

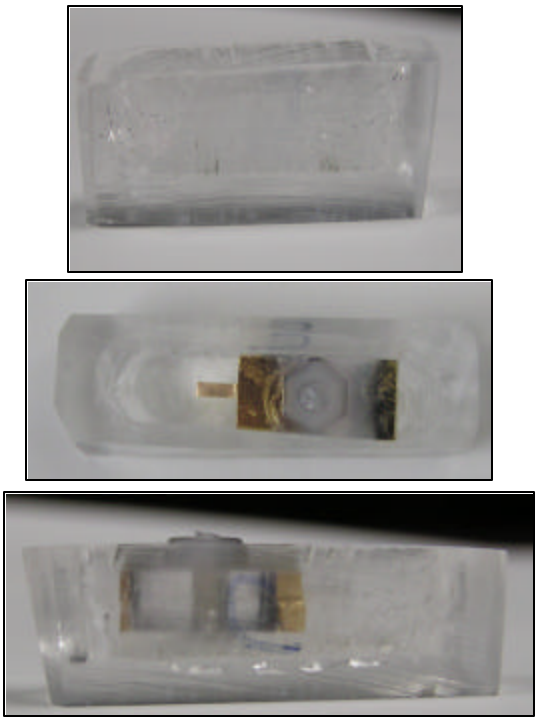

Figure 4.4: Picture of PMMA polymer crucible and cantilever inside crucible

4.2 Microcantilever Preparation for Blood Testing

Before testing a single microcantilever was plasma cleaned for one minute with the PLASMOD plasma cleaner (March Instruments, Inc., Concard, Ca). The plasma cleaner released the cantilever from any debris that could be on the gold surface. The cantilever was then tested to determine its resonance frequency of the gold-coated cantilever. After the resonance frequency of the gold-coated cantilever was measured, the magnetostrictive microcantilever was placed in a PMMA crucible. The crucible was filled with Neutr Avidin™ Biotin-Binding Protein (Pierce Biotechnology, Rockford, IL),

which will be used to immobilize biotinylated protein G. Neutr Avidin^{TM} is known for its ultra-low nonspecific binding and high specificity for biotin binding. The cantilever was then completely submerged in approximately 550µL of Neutr Avidin™. The cantilever stayed in the crucible for two hours to guarantee binding of the Neutr Avidin™ to the gold surface. After two hours, the cantilever was removed from the crucible, rinsed with distilled water, and air-dried. Then the cantilever was placed in the pick-up coil again for measurement. Five measurements were taken to insure the cantilever was placed in the same location (the cantilever was removed and placed back in the pick-up coil between each measurement). The cantilever's crucible was rinsed with distilled water and air-dried. The cantilever was placed back into the crucible and submerged with ImmunoPure® Biotinylated Protein G (Pierce Biotechnology, Rockford, IL). Protein G was used because it binds well to immunoglobulins (antibodies). The same amount of Protein G (550µL) was deposited into the crucible to submerge the entire cantilever. The cantilever was submerged in protein G for two hours to ensure protein G absorption on Neutr Avidin™. The cantilever was taken out of the crucible after two hours, rinsed with distilled water, and air-dried. The cantilever was placed in the pick-up coil for resonance frequency measurement. After five measurements, the cantilever was placed in the rinsed crucible and submerged with Anti-A or Anti-B Murine Monoclonal (Immucor Inc., Norcross, GA). The cantilever was covered in antibody A or B for 1.5 hours. After 1.5 hours, the cantilever was rinsed again with distilled water and placed in the pick-up coil for measurement. After five measurements, the cantilever was placed back again in the rinsed crucible and covered with 550µL of either reagent red blood cells A or reagent red blood cells B (Immucor Gamma, Norcross, GA). The cantilever was left in the blood

cells for 20 minutes before being taken out and rinsed with distilled water. The cantilever was placed in the pick-up coil one last time for five measurements. Blood type was dependent on which antibody was placed on the cantilever's surface. If antibody-B was placed on the cantilever then the antibodies will only grab onto B blood cells. This would increase the mass load of the cantilever and cause the resonance frequency to shift. Figure 4.5 is a brief summary of the cantilever preparation for blood testing. Figure 4.6 is a schematic of the different layers put on the microcantilever in order for it detect red blood cells.

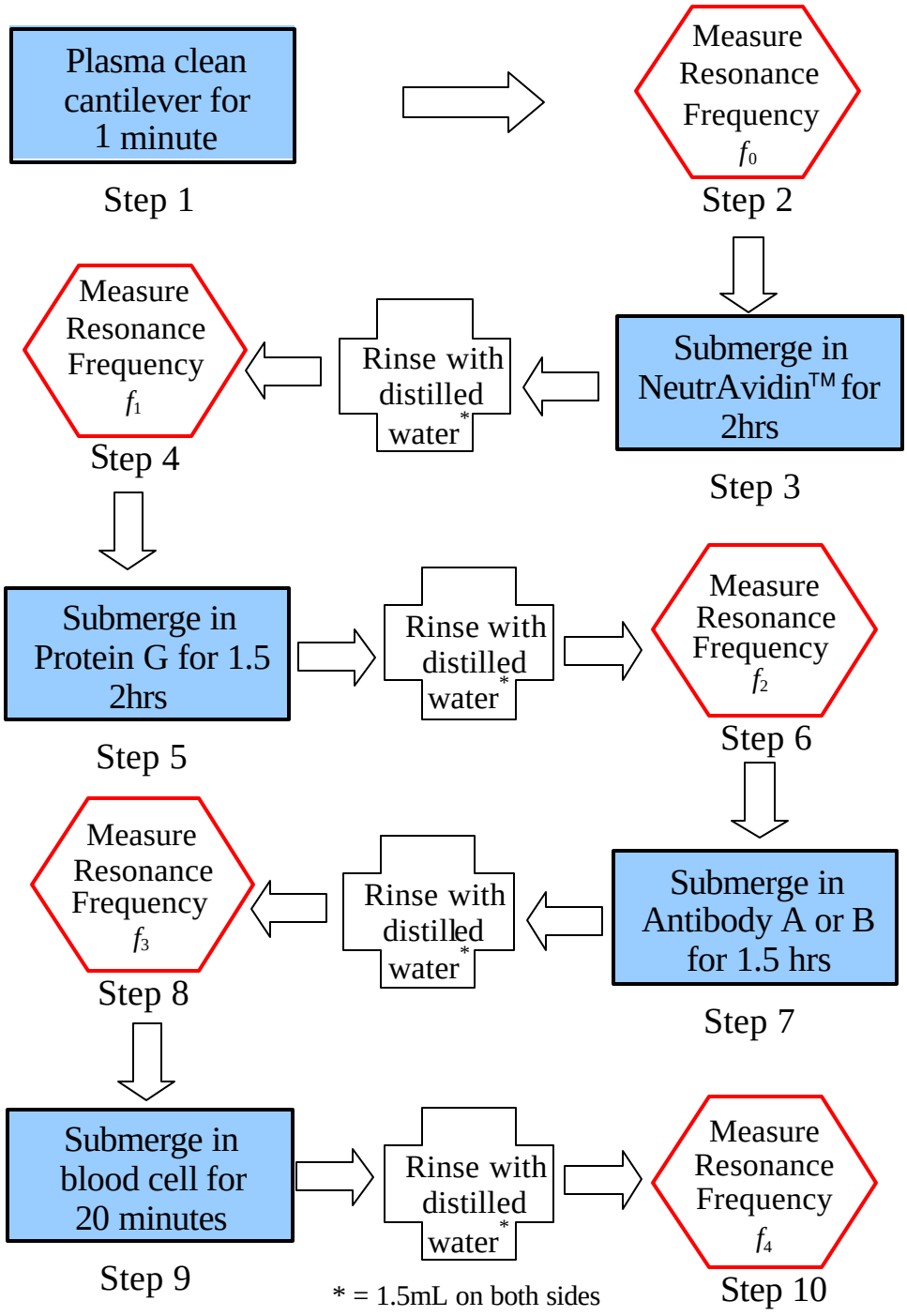

Figure 4.5: Summary of cantilever preparation for blood testing

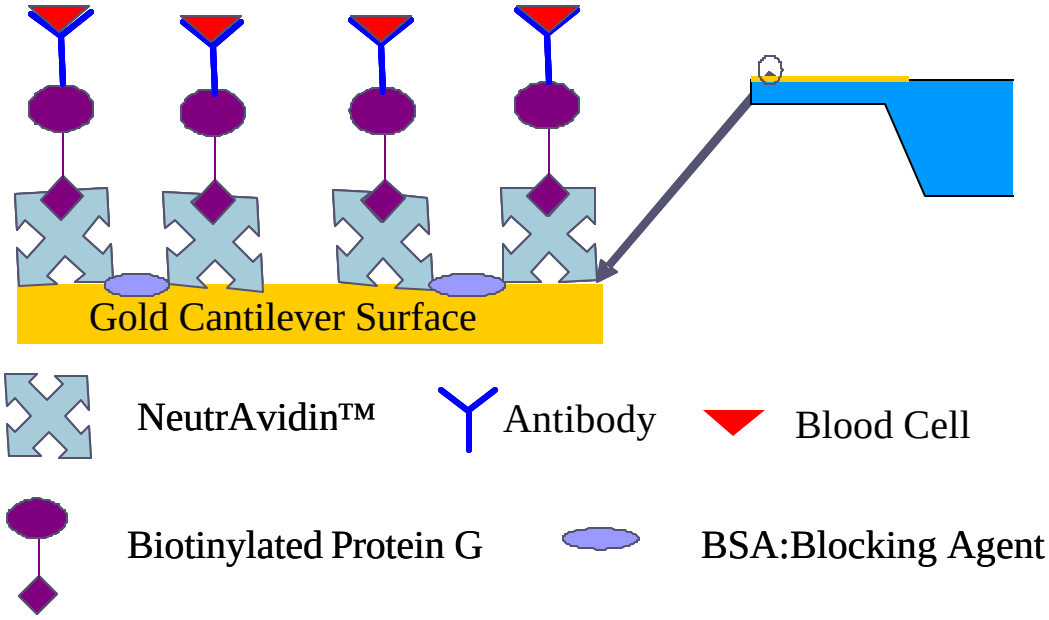

Figure 4.6: Different layers applied to cantilever surface

4.3 Magnetostrictive Thin Film

Glass slides of 2.5x2 cm^2 were used as substrates. Each one was put into a 10:1 water acid solution (10 parts water (volume): 1 part nitric acid (volume)) over night to be cleaned. Once the samples had been cleaned over night, they were taken out of the water: acid solution and dried with nitrogen gas. The glass slides were then taken to the DC/RF sputtering room where the samples were taped onto a plate. The plate was put into a vacuum chamber and the samples were sputtered with chrome and gold. Chromium was sputtered first on the glass slide because it acted as an adhesion layer. The chromium was sputtered for 120 seconds to produce a thickness of about ~100nm. The gold was sputtered for 120 seconds to produce a thickness of about ~200nm. During sputtering the

samples were rotated to ensure a uniform layer of gold and chromium. Gold acted as the electrode in the electrochemical deposition. Once this was completed, the vacuum chamber was vented and the samples were taken out and removed. At this point, the samples were ready to have a thin film deposited on them.

Iron boron was chosen as the magnetostrictive material. The deposition process started by developing the iron boron solution (FeB). The following amount of chemicals to make 100mL of the iron boron solution is given in Table 4.2.

Table 4.2: Iron Boron Chemicals Used for 100mL Solution

Chemicals	Amount
Iron Sulfate ($FeSO_4$-$7H_2O$)	1.999g
Potassium Tetrahydridoborate (KBH_4)	1.5995g
Sodium Hydroxide (NaOH)	1.6g
Potassim Sodium Tartrate ($KNaCH_4O_6$-$4H_2O$)	9.0003g

Once the chemicals were weighed, they were mixed to make the solution. First, the potassium sodium tartrate was placed into a 250mL beaker and 95mL of distilled water was poured into the beaker. The solution was mixed together with a glass-stirring rod until the potassium sodium tartrate completely dissolved into the distilled water. While the potassium sodium tartrate was being dissolved, the sodium hydroxide was placed in 10 ml beaker and 5ml of distilled water was added. The sodium hydroxide was dissolved into the water by gently shaking the beaker. After the potassium sodium tartrate was dissolved, small amounts of iron sulfate were added and mixed into the solution until they completely dissolved. The iron sulfate transformed the clear solution to a brown

color. Next, the dissolved sodium hydroxide was mixed into the solution. Finally, potassium tetrahydridoborate was mixed into the solution until it completely dissolved. The overall appearance of the solution was a dark green color. The solution was then transferred into two 50mL flasks. The electrochemical plating deposition was now ready to be set-up. Figure 4.7 is a flow chart for the construction of the iron boron (FeB) solution.

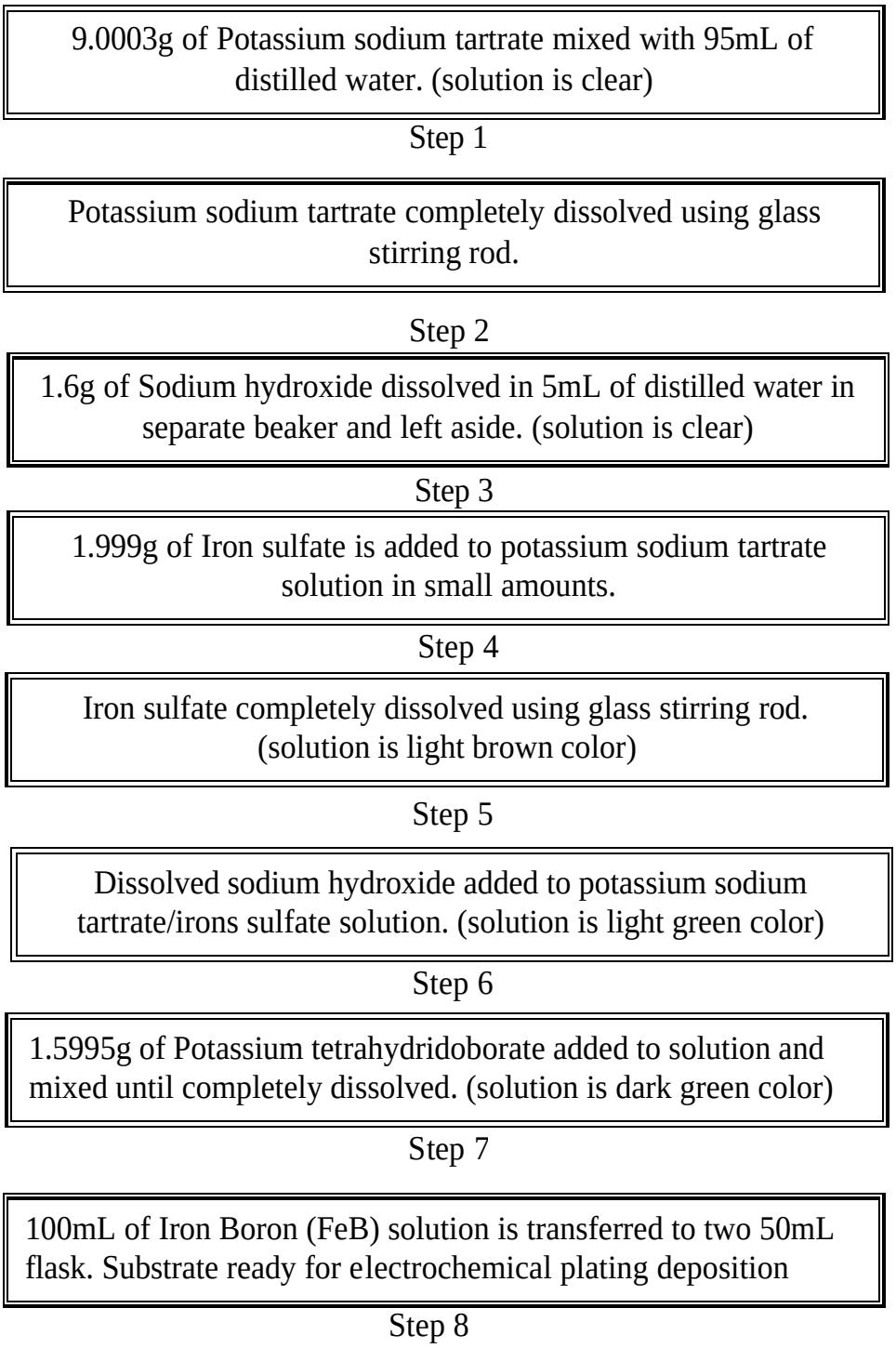

Figure 4.7: Flow chart for construction of iron-born solution

The Epsilon^{TM} electrochemistry analysis network from Bioanalytical System, Inc. was employed to precisely control the deposition process. For precise control, three electrodes were used: working electrode (substrate coated with conductive layer), Counter electrode (platinum mesh), and a reference electrode (standard Ag/AgCl). The configuration of this set up is shown in Figure 4.8.

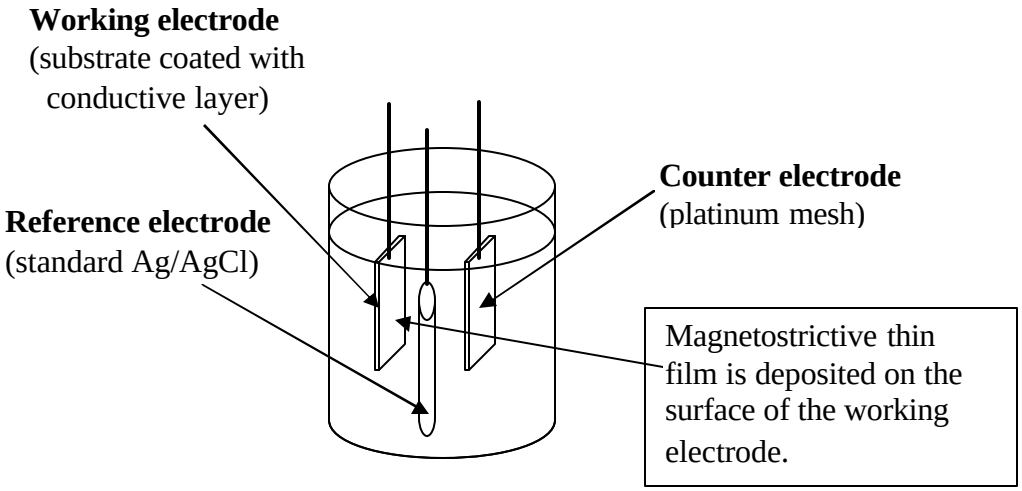

Figure 4.8: Schematic of electrochemical deposition of thin film

The magnetostrictive thin film was deposited on the surface of the working electrode. Table 4.3 shows the deposition parameters used in this research.

Table 4.3: Parameters for electrochemical deposition

Variables	Parameters
Current Density	2-10 mA/cm^2
Deposition Time	30-120 min
Status of Solution	Fresh or Used
Temp. of Deposition	Room Temp. or Temp. Controlled
Concentration of Solution	Regular or Reduced
Magnetic Stirrer	Used or Not Used in Deposition

The current density is defined in this thesis and everywhere else as the amount of current applied per unit area to the substrate. Once the sample was deposited, it was removed from the electrochemical bath, rinsed with distilled water, and dried with nitrogen gas. The start time, current, temperature, and status of solution (whether it was fresh or used) were recorded in notebooks. The deposited sample was taken to the microscope laboratory and pictures were taken at the nine locations, shown in Figure 4.9.

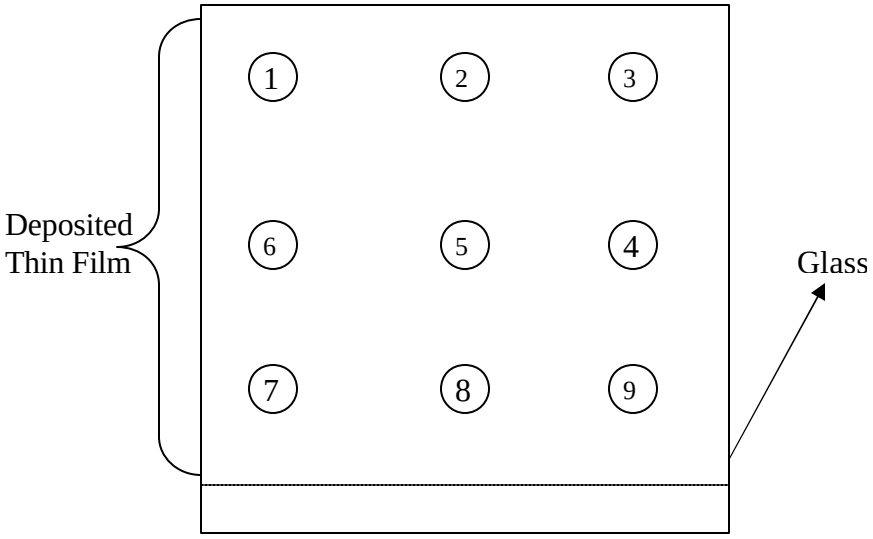

Figure 4.9: Location of pictures taken on thin film

4.4 Fabrication of Thin Film-Subtractive Etching

Before the fabrication of the samples, characterization of the thin film was performed by measuring the thickness of the film using a profilometer. Next the samples were spin coated with a layer of AZ5214-E photoresist. Since the device to spin coat the samples is designed for silicon wafers, each of the samples were attached to a silicon wafer which would act as a holder while they were spin coated. The samples were spin coated for 30

seconds at 3000 rpm. After spin coating, the samples were immediately placed on a hot plate and baked at 105°C for 1 minute. The sample was then taken to the microfabrication machine. A mask containing two different sizes of particles was placed in the machine. The samples were loaded into the machine and the mask was placed on top of each sample, UV light was exposed to the sample for 4 seconds. The photoresist was patterned into either 300µm x 60 µm size particles or 130µm x 30 µm size particles. The samples were then taken to a dark room for developing. The developer AZ 400K^{TM} was mixed with water (1 part developer (volume): 2 parts water (volume)). The samples were immersed in the developer solution for one minute. The sample were then rinsed with water and dried with compressed air. To ensure complete patterns, the pattern of the sample was observed under the microscope. Now the samples were ready to be etched. Figure 4.10 is a schematic of the subtractive etching process.

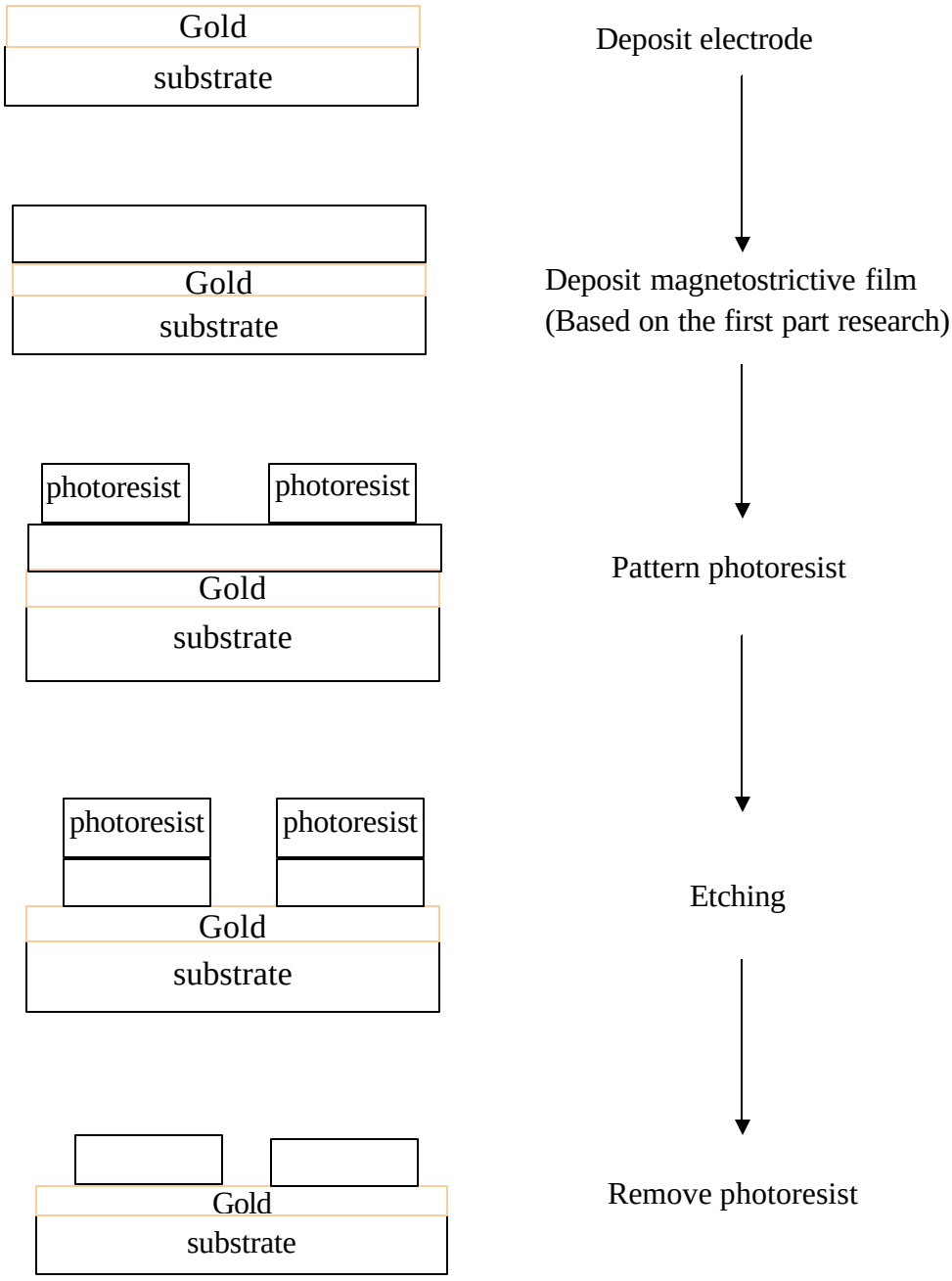

Figure 4.10: Schematic of subtractive etching

In subtractive etching, to remove the non-pattern magnetostrictive film, the samples were etched in a solution of water and nitric acid (10 parts water (volume):1 part acid (volume)). While the solution was being stirred with a magnetic stirrer the samples were immersed in the solution for 2-4 seconds. The samples were then rinsed in distilled water and dried with nitrogen gas. The samples were finally rinsed with ethanol to remove any excess photoresist and dried again with nitrogen gas. The samples were finally taken to the microscope laboratory and pictures in the same nine locations were taken to observe the sensors.

5. RESULTS AND DISCUSSIONS

5.1 Magnetostrictive Microcantilevers

As stated in chapter three, the theoretical resonance frequency for microcantilevers can be determined by equation (3.1).After the cantilevers were clamped with a PMMA holder, but before they were sputtered with chromium and gold, the experimental resonance frequency of the Metglas™/copper film was measured and compared with theoretical resonance frequency. Table 5.1 lists the theoretical resonance frequency, the experimental frequency and length of the cantilever for Figures 5.2 through 5.5. These figures are located at the end of the section.

Table 5.1: Resonance behavior of naked magnetostrictive microcantilever

Figure	Length of Cantilever	Theoretical Resonance Frequency	Experimental Resonance Frequency	Q-value
5.1	3.49 mm	1679.46 Hz	1642.23 Hz	141.59
5.2	2.61mm	3002.88 Hz	2905.45 Hz	115.44
5.3	3.63mm	1550.70 Hz	1460.61 Hz	205.25
5.4	2.90mm	2432.33 Hz	2572.85 Hz	100.25

The percent error between the theoretical resonance frequencies and the experimental resonance frequencies are all within +/- 5%. As was stated in chapter 3, there is a relationship between the cantilever length and resonance frequency. The resonance

frequency decreases with increasing cantilever length. From Table 5.1 it can be seen that the experimental resonance frequency follows that relationship.

5.2 Sensitivity of Microcantilevers

If the mass is loaded uniformly on the surface of the cantilever, the mass sensitivity can be calculated using the change in resonance frequency. When the cantilever was sputtered with chromium and gold, the added mass was assumed to be uniform. Therefore, the mass sensitivity can be calculated theoretically and compared with the experimental results. To calculate the experimental mass sensitivity, equation (3.2) was used. Since the length, width, and thickness of the cantilever are known before it is gold sputtered, the mass load can be calculated. Once the mass load is determined it is used with the observed change in resonance frequency to calculate the mass sensitivity. To calculate the theoretical mass sensitivity, equations 3 and 4 were used. Table 5.2 lists the theoretical and experimental results of the mass sensitivity of the cantilever coated with gold.

Table 5.2: Mass Sensitivity Calculations

Fig.	L	W	Mass load	?*f*	Theo. S_m	Exp. S_m
5.1	3.49mm	0.097mm	63.72 µg	182.1 Hz	0.998 Hz/µg	2.83 Hz/µg
5.2	2.61mm	1.291mm	26.07 µg	72.4 Hz	1.806Hz/µg	2.77 Hz/µg
5.3	3.63mm	1.405mm	35.72 µg	22.8 Hz	0.616 Hz/µg	0.638 Hz/µg
5.4	2.90mm	1.343mm	27.03 µg	52.4 Hz	1.264Hz/µg	1.943 Hz/µg

The percent error between the theoretical mass sensitivities and the experimental mass sensitivities range from +/- 3% to +/-64%. This could be due to the mass not being loading uniformly and the gold coating of the cantilever may also not be uniform. When

the cantilever is sputtered with gold the part of the cantilever that is closest to the PMMA holder may have a different thickness then the free standing part of the cantilever. This is because the cantilever is being rotated on a plated while being coated with gold. A schematic of sputtering the cantilever is shown in Figure 5.1. The cathodes marked 2 and 3 are the different positions of the cathode while the cantilever is being rotated. If the mass is not load uniformly then the experimental data will differ greatly from the theoretical data. This is one reason why the percent error was so great.

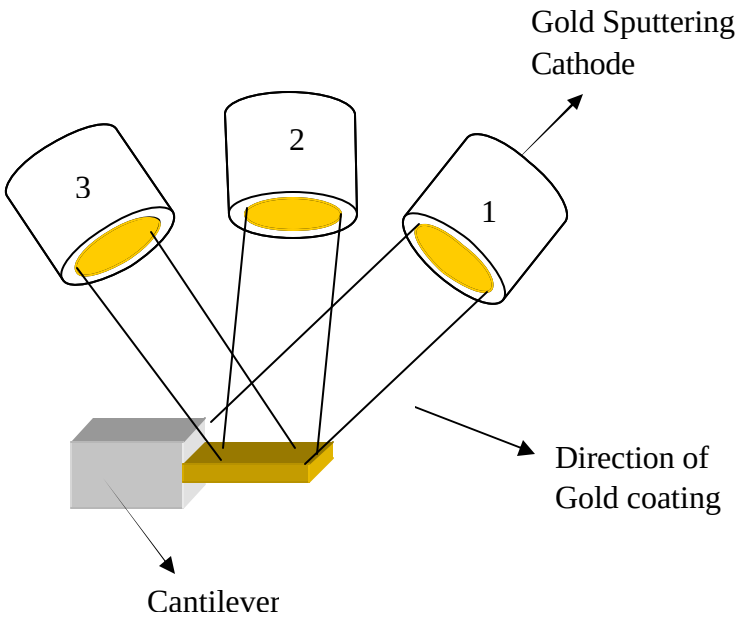

Figure 5.1: Schematic of Gold Coating Cantilever

5.3 Magnetostrictive Microcantilever Biosensor

5.3.1 Positive Results

Dynamic mode cantilevers operate by inducing a resonance frequency shift due to changes in the mass load on the cantilever surface. Therefore by adding layers of Neutr Avidin™, protein G, antibody, and blood cells, detecting a resonance frequency shift is highly plausible. As can been seen from Figure 4.1, after adding 550µL of Neutr Avidin™ to the cantilever, the resonance frequency shifted by 6.6 Hz. The next layer added to the sensor surface was biotinylated protein G; since Neutr Avidin™ is known for immobilizing biotinylated proteins, the biotinylated protein G attached itself to the Neutr- Avidin™. This induced an increase of the cantilever's mass load. This added mass caused another shift in the resonance frequency of 0.9Hz (Figure 5.2). The next layer added to the cantilever surface was the antibody either specific or not specific to the blood cell. In this particular test, antibody B was added first followed by blood cell B. Since protein G is known to bind well to immunoglobulins (antibodies), the antibody attached itself to the biotinylated protein G. Again this added mass caused an additional shift in resonance frequency of 1.4Hz as shown in Figure 5.2. Since antibody B was added before the B blood cells the B blood cells were attracted to the antibody. Thus, the blood cells attached themselves to the antibody B that in turn induced and increase to the cantilever's mass. The schematic of the different layers was shown in Figure 4.6 on page 49. The data shown in Figures 5.3 and 5.4 also consists of adding antibody B and blood cell B to the cantilever's surface. Tables 5.3 – 5.6 contain the experimental mass sensitivity (Sm) of the cantilevers calculated from equation (3.2). If the mass loading was

uniform we could calculate to total amount of mass added to the cantilever surface after each layer.

Table 5.3: Calculations due to frequency shift

Figure 5.2		
Layers	**Sensitivity**	**Frequency Shift**
Gold	$1.00\frac{mg}{Hz}$	0 Hz
Neutr Avidin™		6.6 Hz
Protein G		0.9 Hz
Antibody B		1.4 Hz
Blood Cell B		2.7 Hz

Table 5.4: Calculations due to frequency shift

Figure 5.3		
Layers	**Sensitivity**	**Frequency Shift**
Gold	$0.554\frac{mg}{Hz}$	0 Hz
Neutr Avidin™		14.3 Hz
Protein G		2.1 Hz
Antibody B		15.7 Hz
Blood Cell B		13.3 Hz

Table 5.5: Calculations due to frequency shift

Figure 5.4		
Layers	**Sensitivity**	**Frequency Shift**
Gold	$1.623\frac{mg}{Hz}$	0 Hz
Neutr Avidin™		28.1 Hz
Protein G		4.5Hz
Antibody B		7.7 Hz
Blood Cell B		14.7 Hz

Figure 5.5 shows the results of adding antibody B to the sensor surface followed by blood cell A. Since the cantilever contained B antibodies, the A blood cells did not have an attraction to the antibodies. Therefore, it seems none or minute amounts of the A blood cells attached themselves to the antibodies. As was stated in chapter three the fitting of the data could be out ±0.3 Hz. This non-attraction of the blood cells to the cantilever's surface should cause the mass of the sensor to remain unchanged, which would cause the resonance frequency shift to remain unchanged. It can be seen in Figure 5.5 that there was a shift in resonance frequency for the layers of Neutr Avidin™, protein G, antibody B but there was a minute shift in frequency for blood cells A. The following table contains the experimental mass sensitivity of the cantilever (Figure 5.5) calculated from equation (3.2). If the mass loading was uniform we could calculate to total amount of mass added to the cantilever surface after each layer.

Table 5.6: Calculations due to frequency shift

Figure 5.5		
Layers	**Sensitivity**	**Frequency Shift**
Gold	$0.791\frac{mg}{Hz}$	0 Hz
Neutr Avidin™		21.7 Hz
Protein G		2 Hz
Antibody B		1.8 Hz
Blood Cell A		0.3 Hz

For future experiments, utilizing a blocking agent on the cantilever's surface is one way to ensure positive results. When a blocking agent is applied on the surface of a sensor, chances of non-specific binding is reduced. If a blocking agent is added to an

experiment the shift in resonance frequency can be attributed to specific binding to the surface of the cantilever.

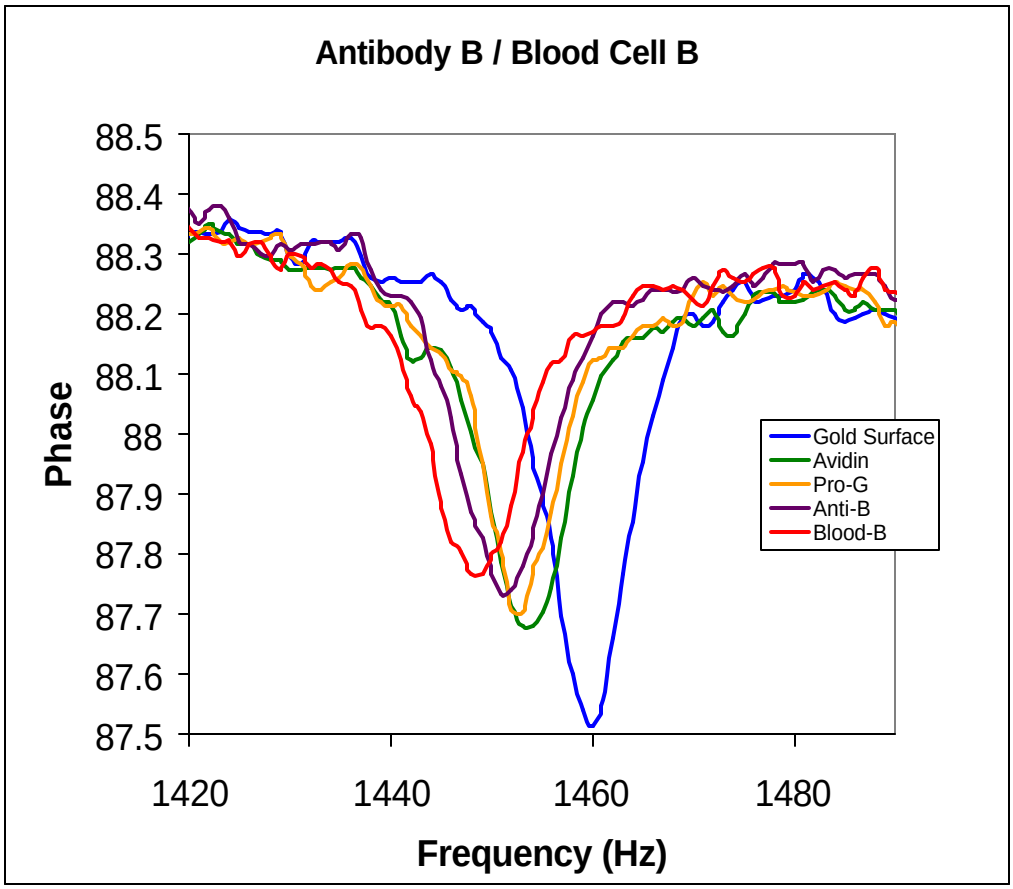

Figure 5.2: Frequency Shift due to mass loading

	Time	Avg. Frequency	Avg.Frequency Shift
Gold		1460.1±0.62 Hz	0±0.62 Hz
Avidin	2 hrs	1453.5±1.19 Hz	6.6±1.19 Hz
Protein G	2 hrs	1452.6±1.72 Hz	0.9±1.72 Hz
Antibody B	1.5 hrs	1451.2±0.93 Hz	1.4±0.93 Hz
Blood B	20 min	1448.5±0.77 Hz	2.7±0.77 Hz

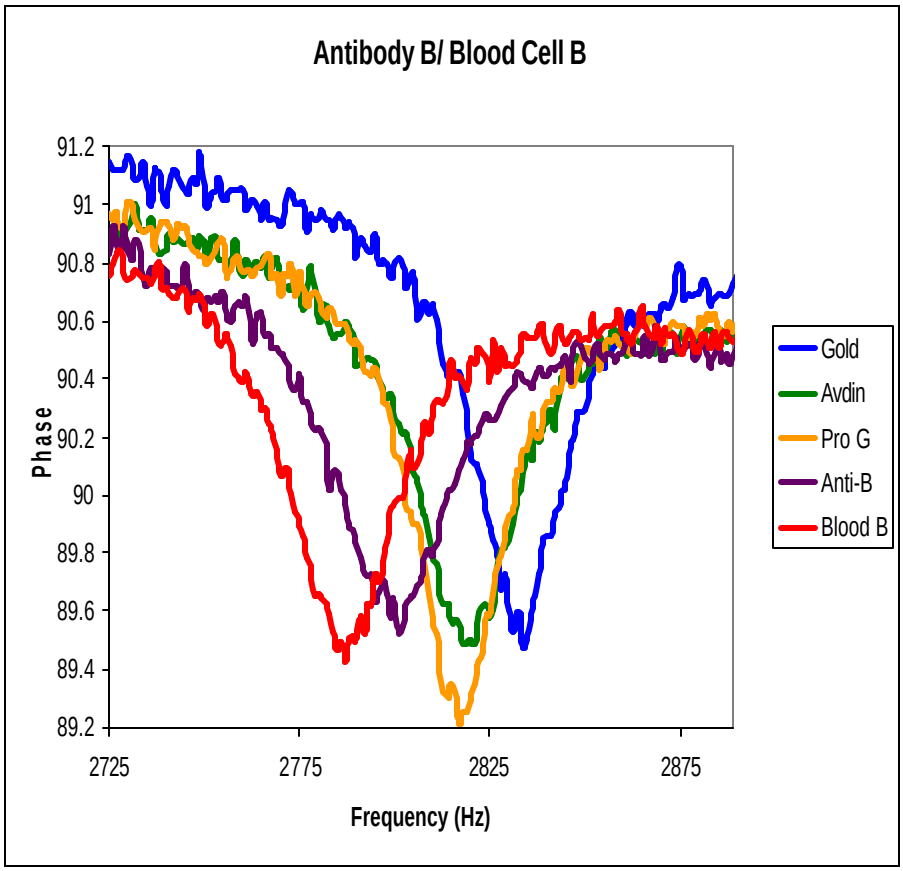

Figure 5.3: Frequency Shift due to mass loading

	Time	Avg. Frequency	Avg.Frequency Shift
Gold		2833±0.76 Hz	0±0.76 Hz
Avidin	2 hrs	2818.7±1.15 Hz	14.3±1.15 Hz
Protein G	2 hrs	2816.6±1.90 Hz	2.1±1.90 Hz
Antibody B	1.5 hrs	2800.9±1.37 Hz	15.7± 1.37 Hz
Blood B	20 min	2787.6±0.96 Hz	13.3±0.96 Hz

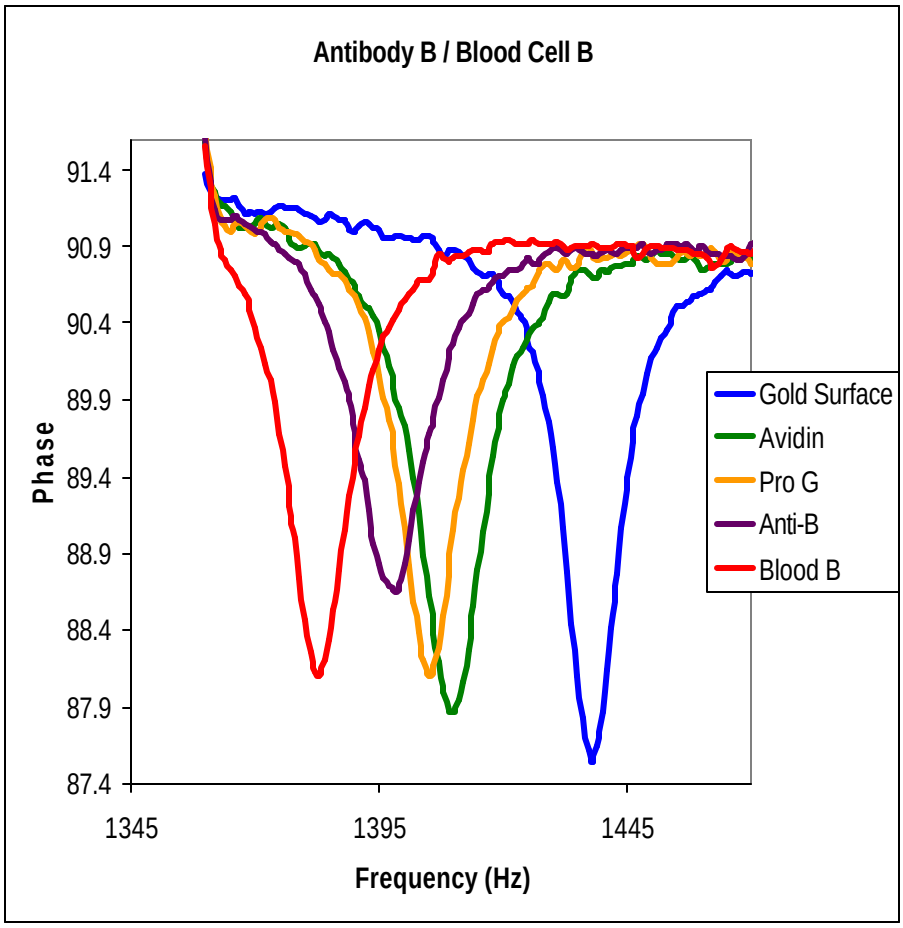

Figure 5.4: Frequency Shift due to mass loading

	Time	Avg. Frequency	Avg.Frequency Shift
Gold		1437.8± 1.48 Hz	0± 1.48 Hz
Avidin	2 hrs	1409.7±1.02 Hz	28.1±1.02 Hz
Protein G	2 hrs	1405.2±0.91 Hz	4.5±0.91 Hz
Antibody B	1.5 hrs	1397.5±1.30 Hz	7.7±1.30 Hz
Blood B	20 min	1382.8±1.12 Hz	14.7±1.12 Hz

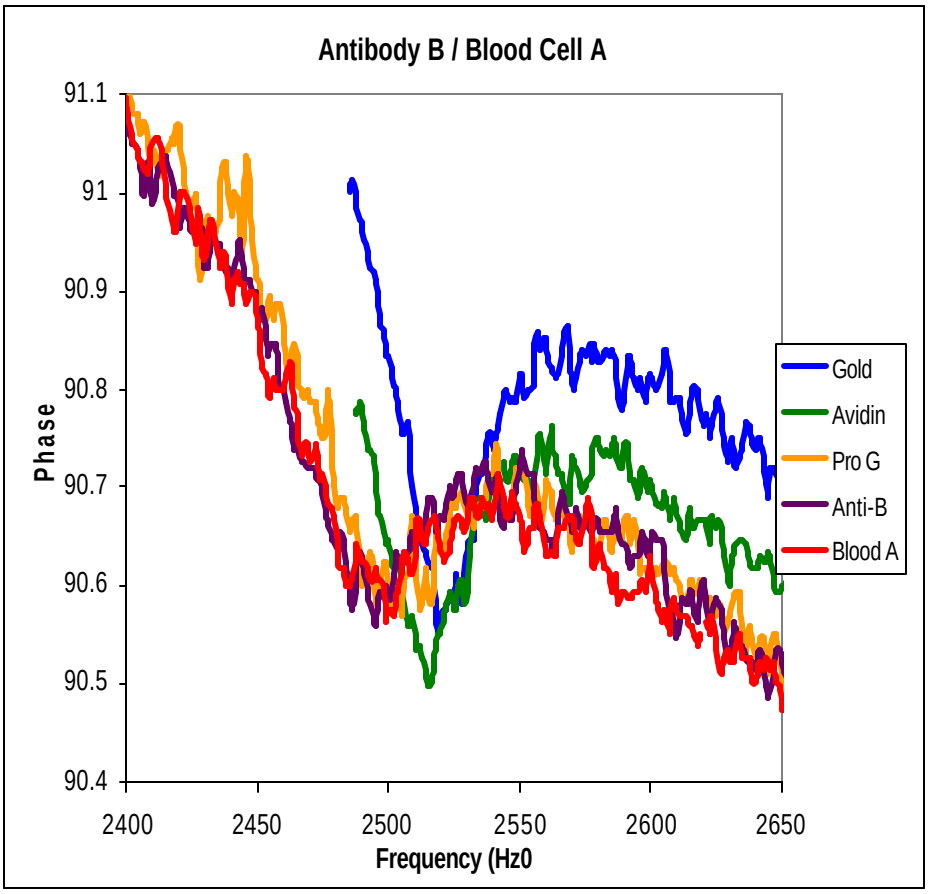

Figure 5.5: Frequency Shift due to mass loading

	Time	Avg. Frequency	Avg.Frequency Shift
Gold		2520.4±1.45 Hz	0±1.45 Hz
Avidin	2 hrs	2498.7±1.34 Hz	21.7±1.34 Hz
Protein G	2 hrs	2496.7±1.02 Hz	2.0±1.02 Hz
Antibody B	1.5 hrs	2494.9±0.99 Hz	1.8±0.99 Hz
Blood A	20 min	2494.6±1.19 Hz	0.3±1.19 Hz

5.3.2: Magnetostrictive Microcantilever Sensors: Issues related to reproducibility

Figures 5.6 and 5.7 are tests that showed unexpected results. After adding certain layers, the resonance frequency shifted in the wrong direction. In Figure 5.6 after, the Neutr Avidin™ was added to the cantilever's surface, the resonance frequency increased 27 Hz. There are several explanations on why this occurred and what can be done to circumvent these problems. The following points will be addressed on why the cantilevers may have not worked properly.

- Cleaning Process
- Sputtering System

One of the biggest factors that may have caused failed results was the cleaning process. The cantilever was handled many times by hand when it was tested after each layer as was shown in chapter 4. Continuously taking the cantilever out of the crucible, rinsing it, and letting it air dry provides opportunities for debris to attach/unattach itself to the cantilever. If debris had attached itself to the surface of the cantilever, when the debris is rinsed away the mass of cantilever will decrease. This would cause the resonance frequency to increase. One way to solve this problem is to set-up a flow system that goes through the pick-up coil so that the cantilever can stay in one place. This would allow fewer hands on the cantilever and would decrease the chances of debris attaching itself to the surface of the cantilever.

Another reason for negative results could be the quality and adhesion of gold layer on cantilevers, which was deposited using a DC sputtering system. If the any of the gold comes off the cantilever during the experiment, the mass of the cantilever will

decrease which would result in an increase in the resonance frequency. This may be the cause for failure in Figure 5.6.

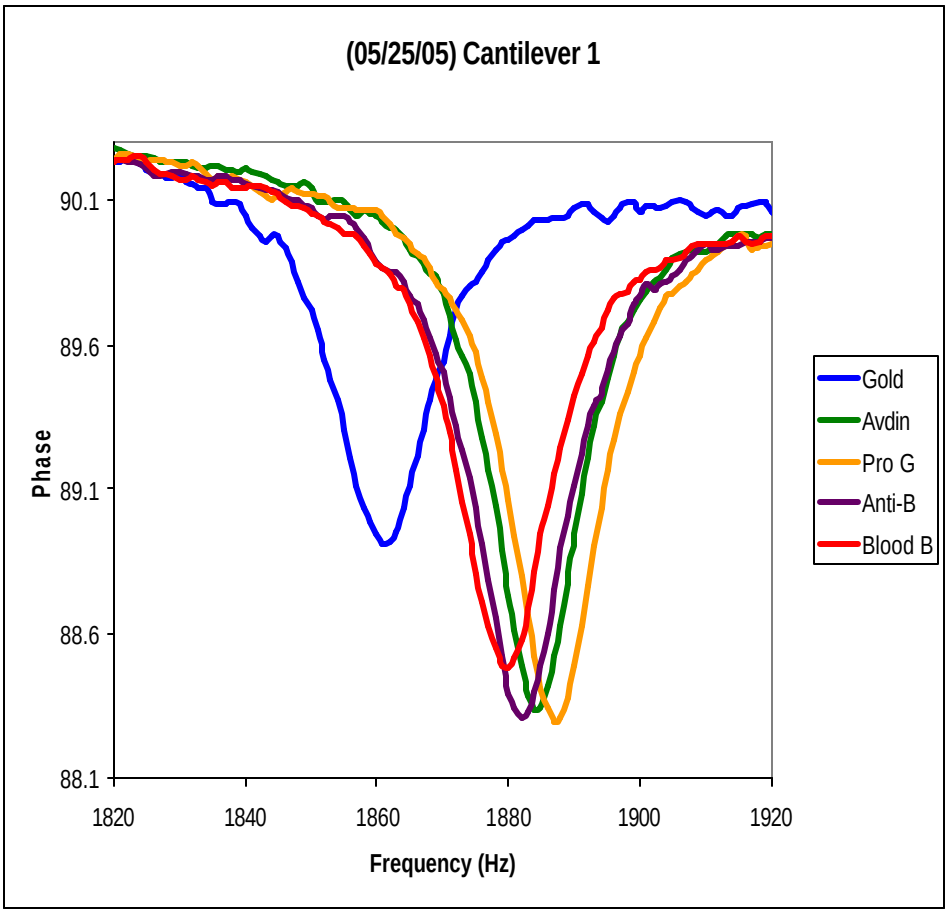

Figure 5.6: Frequency Shift due to mass loading

	Time	Avg. Frequency	Avg.Frequency Shift
Gold		1861.2±1.88 Hz	0±1.88 Hz
Avidin	2 hrs	1887.9±1.79 Hz	26.7±1.79 Hz to right
Protein G	2 hrs	1886.3±0.86 Hz	1.6±0.86 Hz
Antibody B	1.5 hrs	1882.4±1.74 Hz	3.9±1.74 Hz
Blood B	20 min	1880.0±0.38 Hz	2.4±0.38 Hz

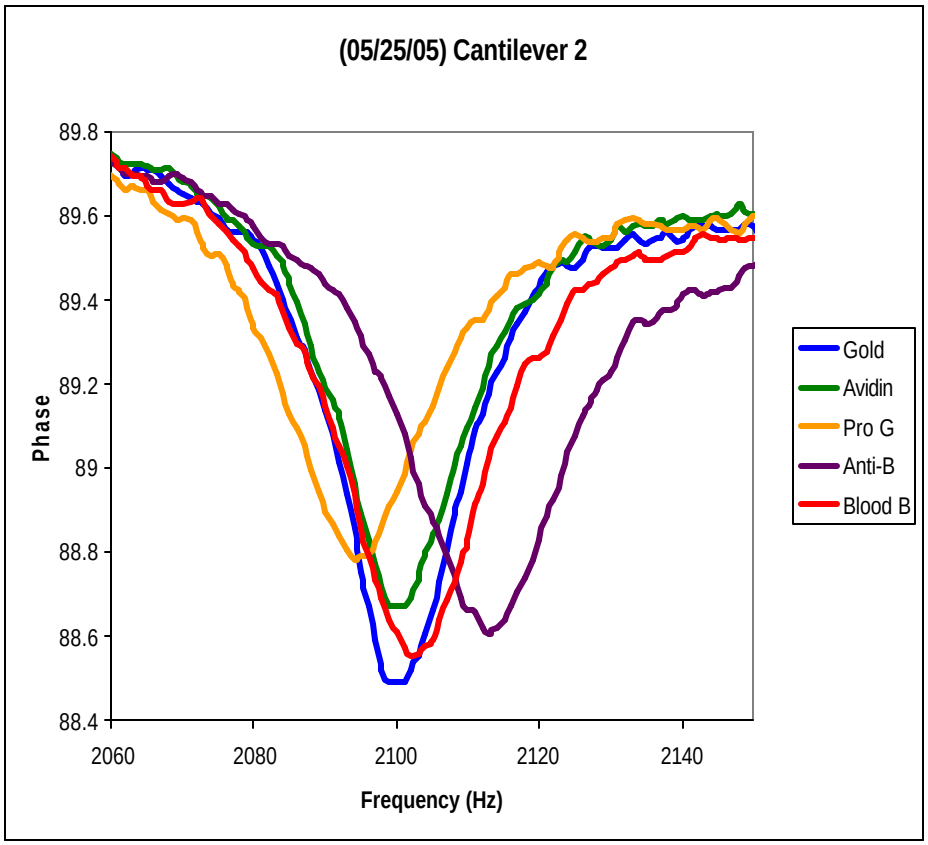

Figure 5.7: Frequency Shift due to mass loading

	Time	Avg. Frequency	Avg.Frequency Shift
Gold		2100.3±1.56 Hz	0±1.56 Hz
Avidin	2 hrs	2101.8±0.88 Hz	1.5±0.88 Hz to right
Protein G	2 hrs	2095.2±1.22 Hz	6.6±1.22 Hz
Antibody B	1.5 hrs	2113.1±0.78 Hz	17.9±0.78 Hz to right
Blood B	20 min	2103.5±1.12 Hz	9.6±1.12 Hz

5.4 Thin Film: Deposition

For the thin film project different combinations were used to determine which one was best suited for deposition. The variables used the in the thin film deposition are listed in Table 5.7.

Table 5.7: Deposition Parameters

Variables	Conditions
Current Density	2-10 mA/cm^2
Deposition Time	30-120 min
Status of Solution	Fresh or Used
Temp. of Deposition	Room Temp. or Temp. Controlled
Concentration of Solution	Regular or Reduced
Magnetic Stirrer	Used or Not Used in Deposition

All of the substrates used in the thin film project were glass. At first, the only variables altered at room temperature were current density, deposition time, and status of solution. The status of the solution was either fresh or used. A fresh solution means no sample has been deposited in that particular solution, while a used solution had already been used to deposit a previous sample. A used solution was only used once. Alternating the different deposition conditions of the variables resulted in non-consistent results. Table 5.8 lists the different deposition parameters used for current density, deposition time, and status of solution.

Table 5.8: Summary of Deposition Parameters

Combination Number	Current Density	Deposition Time	Status of Solution	Temp.	Spots: Heavy	Spots: Light	Bubbles	Cracks: Big	Cracks: Small	Dentrite-Like Formation
1	2 mA/cm^2	30 min	Fresh	RT	NO DEPOSITION					
2	2 mA/cm^2	60 min	Fresh	RT		X				
3	2 mA/cm^2	60 min	Used	RT	X	X				
4	3 mA/cm^2	90 min	Used	RT	X	X				
5	3 mA/cm^2	120 min	Fresh	RT	X					
6	3 mA/cm^2	120 min	Used	RT		X				
7 (4)	3 mA/cm^2	60 min	Fresh	RT	X		X			
	3 mA/cm^2	60 min	Fresh	RT		X	X	X	X	X
	3 mA/cm^2	60 min	Fresh	RT		X				
	3 mA/cm^2	60 min	Fresh	RT	X	X	X		X	X
8 (7)	3 mA/cm^2	60 min	Used	RT		X		X		
	3 mA/cm^2	60 min	Used	RT	X	X		X		
	3 mA/cm^2	60 min	Used	RT	X	X				
	3 mA/cm^2	60 min	Used	RT	X					
	3 mA/cm^2	60 min	Used	RT	X					
	3 mA/cm^2	60 min	Used	RT		X	X			
	3 mA/cm^2	60 min	Used	RT	X		X			
9	4 mA/cm^2	60 min	Fresh	RT	X					
10 (3)	4 mA/cm^2	60 min	Used	RT	X					
	4 mA/cm^2	60 min	Used	RT		X			X	
	4 mA/cm^2	60 min	Used	RT	X		X			
11(3)	5 mA/cm^2	30 min	Fresh	RT	X	X			X	
	5 mA/cm^2	30 min	Fresh	RT	X			X		
	5 mA/cm^2	30 min	Fresh	RT	X					
12	5 mA/cm^2	30 min	Used	RT	X			X		
13	5 mA/cm^2	60 min	Fresh	RT	X				X	X
14	6 mA/cm^2	30 min	Fresh	RT		X			X	
15	8 mA/cm^2	30 min	Used	RT	X				X	
16	10 mA/cm^2	30 min	Fresh	RT	X				X	

As can be seen from Table 5.8 sixteen different combinations of the three variables were used (current density, deposition time, and status of solution) to deposit the magnetostrictive material on a glass substrate. As stated in the experimental section, after deposition, pictures were taken of the substrate at nine different locations to observe the thin film. The problems observed from deposition include the following: heavy spots, light spots, big cracks, small cracks, bubbles and dendrite-like formations. Figures 5.8 through 5.13 represent the problems associated with deposition.

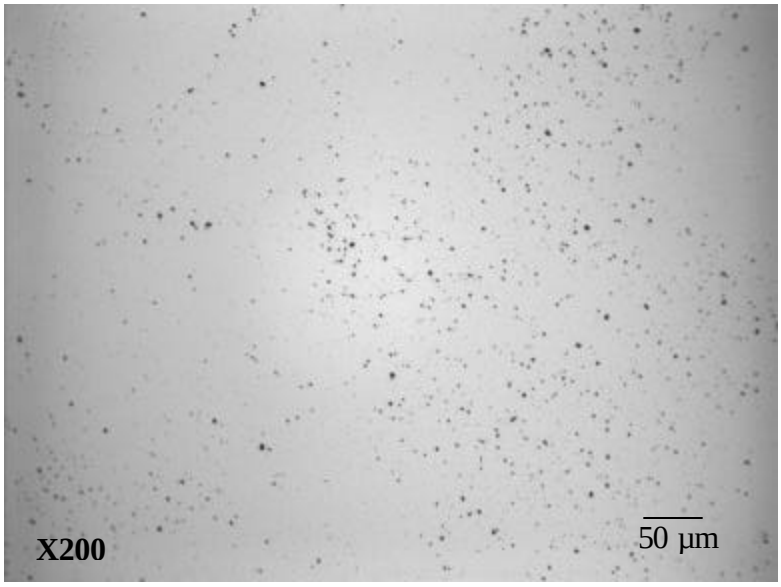

Figure 5.8: Deposition Problem – Heavy Spots

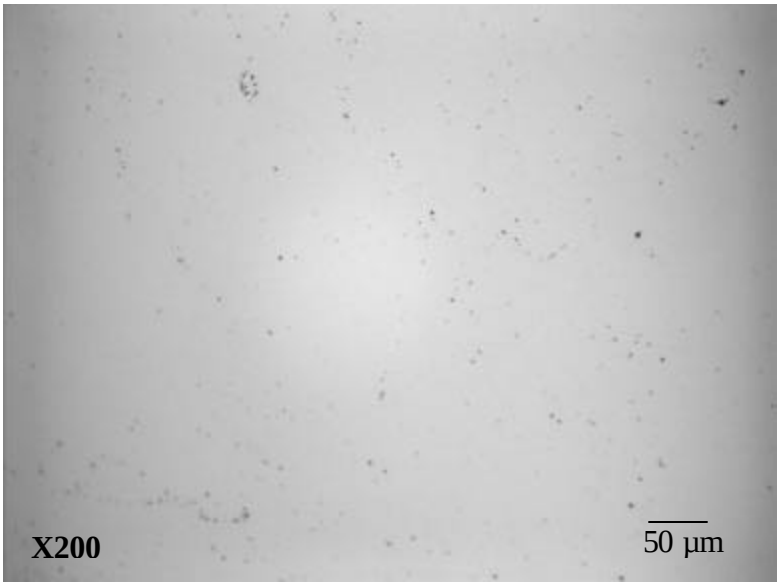

Figure 5.9: Deposition Problem- Light Spots

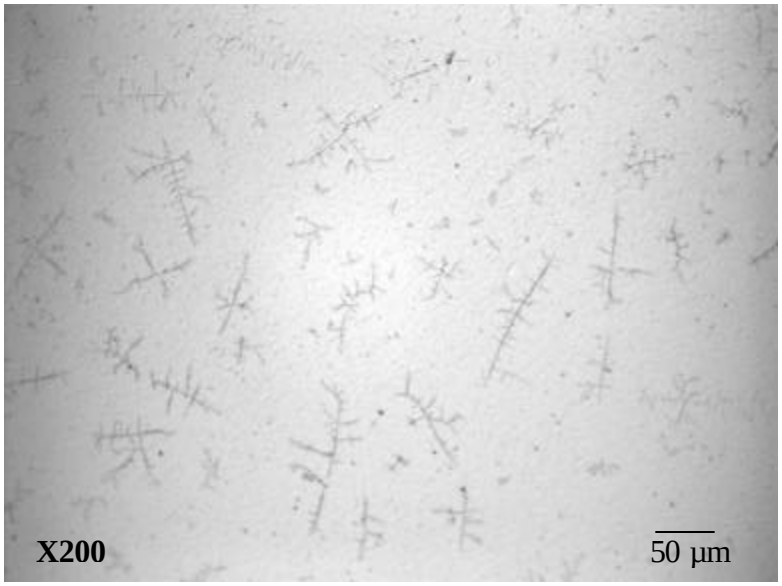

Figure 5.10: Deposition Problem – Dendrite-Like Formation

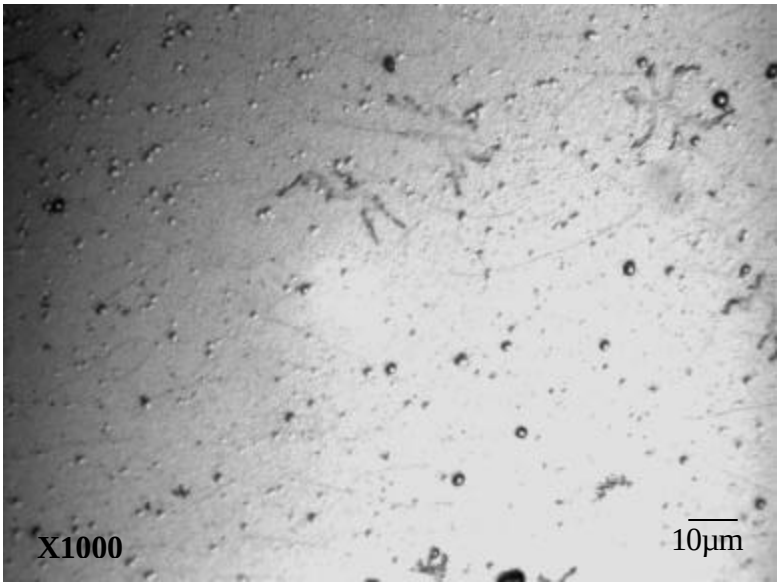

Figure 5.11: Deposition Problem - Bubbles

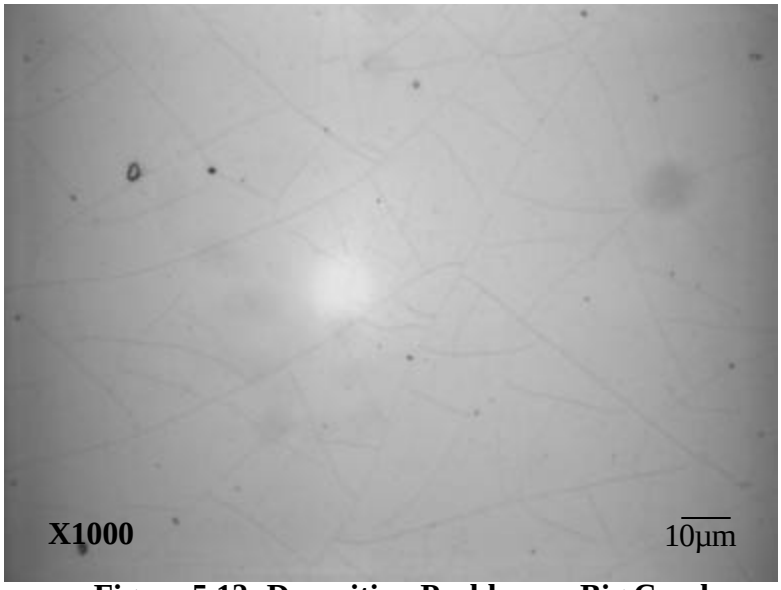

Figure 5.12: Deposition Problems – Big Cracks

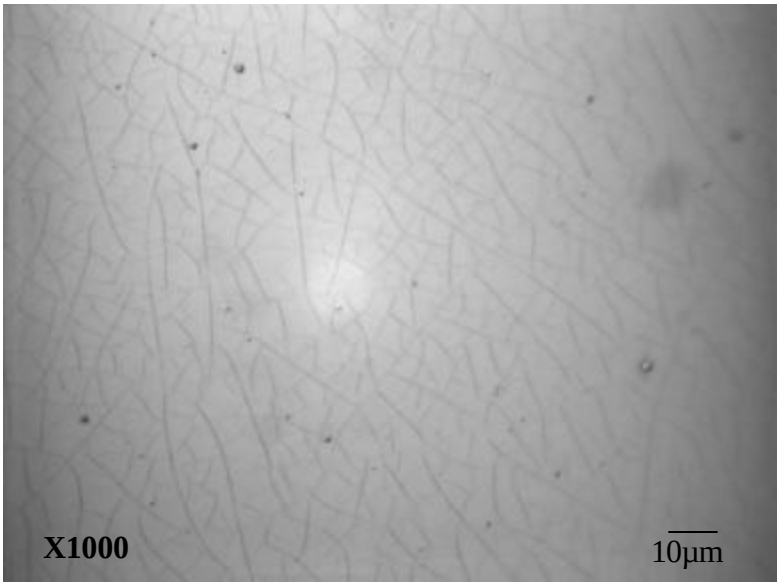

Figure 5.13: Deposition Problems – Small Cracks

Of the sixteen deposition conditions only four conditions were used at least three times. Therefore the deposition results of these parameters will be discussed. Combination 7 contained four samples with the same conditions. After evaluating each thin film, it was concluded that when a glass substrate was deposited at this condition the main problems associated with the majority of the samples were bubbles and light spots. The deposited thin film on half the substrates contained heavy spots, small cracks, and dendrite-like formations. Only one sample contained big cracks. The next deposition combination is combination 8. Seven samples were deposited with this combination. The main problems associated with this condition were heavy spots and light spots. A couple of samples contained bubbles and big cracks. None of the samples contained small cracks and crystal formations. Another deposition combination discussed is combination 10.
Three samples were deposited with combination 10. Over half of the thin film samples contained heavy spots. While half contained light spots, bubbles, and small cracks. None of the samples contained big cracks or dendrite-like formations. The last deposition combination to be discussed is combination 11. Three samples were tested at this condition. All three of samples contained heavy spots. Half of the samples contained light spots, big cracks, and small cracks. None of the samples contained bubbles or dendrite-like formations.

The one problem that was consistent with all the deposition parameters just discussed and even the parameters not discussed were spots. All the samples that were deposited contained either heavy or light spots. These spots are believed to be a result of the cleaning process of the substrates. From the results above to prevent dendrite-like formation on the magnetostrictive thin film combination 8, 10, and 11 could be used. The

rest of the data was too scattered to determine which one would result in cracks or bubbles.

To prevent dendrite-like formation, bubbles, cracks, and spots on the magnetostrictive thin film, three more parameters were added. These variables were added to see if consisted results could be obtained. The following parameters were added: temperature controlled deposition bath, reduced solution concentration, and a magnetic stirrer. The following table contains the additional variables added in the thin film deposition.

Table 5.9: Additional Variables Added to Deposition

Combin. Number	Deposit current	Deposit time	Status of Bath	Diff.	Temp	Spots: Heavy	Spots: Light	Bubbles	Cracks: Big	Cracks: Small	Dentrite-Like Formation
1	2 mA/cm^2	60 min	Fresh	1	~5°C	X				X	
2	2 mA/cm^2	60 min	Used	1	7°C	X		X			
3	3 mA/cm^2	180 min	Used	1	~4°C	X		X		X	
4	3 mA/cm^2	60 min	Fresh	1	7°C	X					
5	3 mA/cm^2	60 min	Used	1	5°C	X				X	
6	4 mA/cm^2	60 min	Used	1	5°C	X					
7	5 mA/cm^2	30 min	Fresh	1	18°C	X				X	
8 (2)	5 mA/cm^2	30 min	Used	1	5°C	X					
	5 mA/cm^2	30 min	Used	1	5°C	X					
9	5 mA/cm^2	60 min	Used	1	5°C		X		X		
10	2mA/cm^2	60 min	Fresh	2	RT	X*		X			
11	2mA/cm^2	60 min	Used	2	RT	X*					
12	2mA/cm^2	120 min	Fresh	3	RT	X*					
13	5mA/cm^2	60 min	Fresh	3	RT	X*		X		X	
14	2mA/cm^2	60 min	Fresh	4	RT	X*		X			
15	2mA/cm^2	120 min	Fresh	4	RT	X*					

* = Very Heavy Spots
1 = Temperature Controlled
2 = Reduced Concentration & Stirrer
3 = Reduced Concentration
4 = Magnetic Stirrer

There was only one deposition parameter that was used twice so more testing has to be completed to determine if these combinations provide positive or negative consistent results. But, from Table 5.9 all of the combinations contained heavy spots. Consequently, the addition of these new variables did not eliminate the spots seen in the earlier deposition parameters.

Since hardly any samples were tested at the same parameters, very little can be stated about what specific parameters worked best. But enough samples were tested using the different variables to give an overall judgment on whether that particular variable did indeed help the overall appearance of the thin film. The first variable listed on the table was the temperature controlled deposition bath. The purpose for controlling the temperature of the solution was to determine if the cracks and spots would disappear. But these substrates contained all but one of the deposition problems (crystal formation). The last three variables included using a magnetic stirrer to stir the solution while the substrate was being deposited, reducing the concentration of the solution, and using a magnetic stirrer with a reduced concentration. Only a couple of samples were tested with these parameters, so it is difficult to give a definite conclusion about the overall effect they had on the thin film. The one thing that seemed to be consistent was large amounts of small spots of the thin films. Figures 5.14 -5.16 show the thin film spots when these parameters are used.

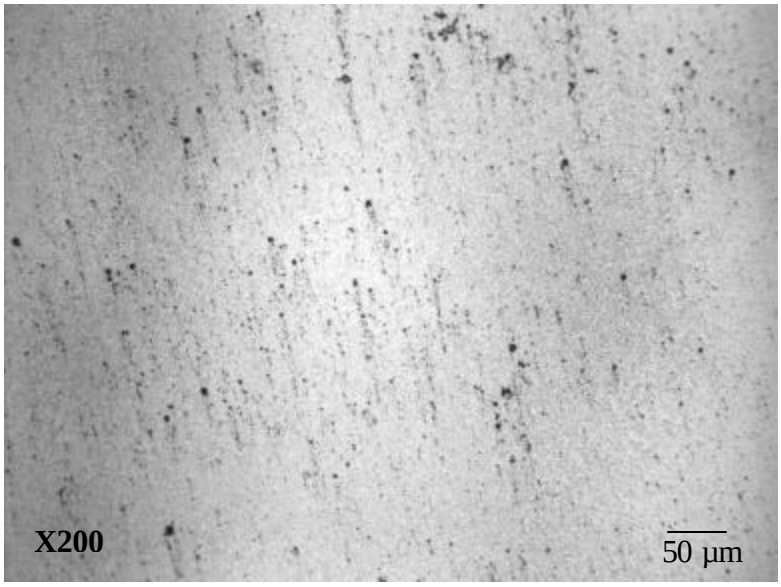

Figure 5.14: Reduced Concentration Thin Film

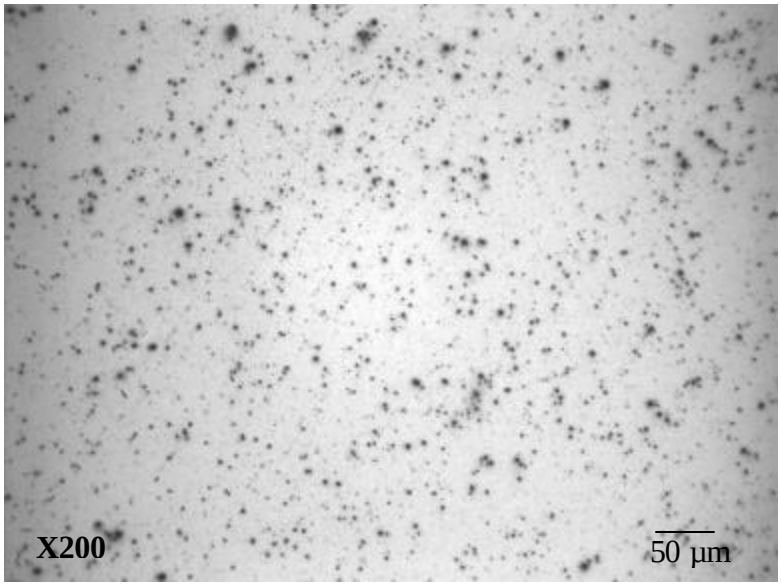

Figure 5.15: Magnetic Stirrer

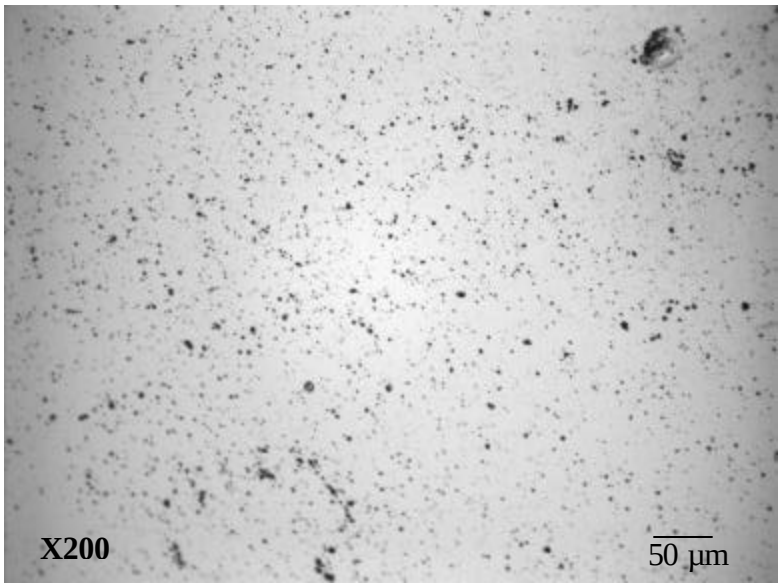

Figure 5.16: Reduced Concentration and Magnetic Stirrer

As can be seen from Figures 5.14- 5.16, the thin film contained a lot more spots than any of the other deposition parameters. None of the samples contained any dendrite-like formation but some samples contained bubbles and cracks. More experiments need to be completed to pinpoint which parameters work best.

Table 5.10: Direct Comparison of First Variables and Added Variables

Combin. #	Current Density	Deposition Time	Status of Solution	diff	Temp.	Spots: Heavy	Spots: Light	Bubbles	Cracks :Big	Cracks :Small	Dentrite-Like Formation
	2 mA/cm^2	60 min	Fresh	0	RT		X				
1	2 mA/cm^2	60 min	Fresh	1	5°C	X				X	
	2 mA/cm^2	60 min	Used	0	RT	X	X				
2	2 mA/cm^2	60 min	Used	1	7°C	X		X			
	3 mA/cm^2	60 min	Fresh	0	RT	X		X			
	3 mA/cm^2	60 min	Fresh	0	RT		X	X	X	X	X
	3 mA/cm^2	60 min	Fresh	0	RT		X				
	3 mA/cm^2	60 min	Fresh	0	RT	X	X	X		X	X
3	3 mA/cm^2	60 min	Fresh	1	7°C	X					
	3 mA/cm^2	60 min	Used	0	RT		X		X		
	3 mA/cm^2	60 min	Used	0	RT	X	X		X		
	3 mA/cm^2	60 min	Used	0	RT	X	X				
	3 mA/cm^2	60 min	Used	0	RT	X					
	3 mA/cm^2	60 min	Used	0	RT	X					
	3 mA/cm^2	60 min	Used	0	RT		X	X			
	3 mA/cm^2	60 min	Used	0	RT	X		X			
4	3 mA/cm^2	60 min	Used	1	5°C	X				X	
	4 mA/cm^2	60 min	Used	0	RT	X					
	4 mA/cm^2	60 min	Used	0	RT		X			X	
	4 mA/cm^2	60 min	Used	0	RT	X		X			
5	4 mA/cm^2	60 min	Used	1	5°C	X					
	5 mA/cm^2	30 min	Fresh	0	RT	X	X			X	
	5 mA/cm^2	30 min	Fresh	0	RT	X			X		
	5 mA/cm^2	30 min	Fresh	0	RT	X					
6	5 mA/cm^2	30 min	Fresh	1	18°C	X				X	
	5 mA/cm^2	30 min	Used	0	RT	X			X		
	5 mA/cm^2	30 min	Used	1	5°C	X					
7	5 mA/cm^2	30 min	Used	1	5°C	X					
	5 mA/cm^2	60 min	Fresh	0	RT	X				X	X
8	5mA/cm^2	60 min	Fresh	3	RT	X*		X		X	

* = Very Heavy Spots
1 = Temperature Controlled
2 = Reduced Concentration & Stirrer
3 = Reduced Concentration
4 = Magnetic Stirrer

As can be seen from Table 5.10 after combining the data together, there was only enough information to make speculations about the first variables at room temperature and the

first variables at a controlled temperature. Overall when the temperature of the deposition bath was controlled the only main problems seen were small cracks and heavy spots. Since very few samples were tested at controlled temperatures, precise judgments can not be made whether a temperature controlled bath guaranteed to eliminate four of the six problems associated with deposition.

5.5: Thin Film: Microfabrication

As stated in the experimental section, for the microfabrication process, all the samples were used with the same parameters. The only difference between the samples depended on the thin film deposition layer. If the substrate contained cracks after deposition, cracks on the sensor pattern would appear. Figures 5.17- 5.23 are some examples of the microfabrication process.

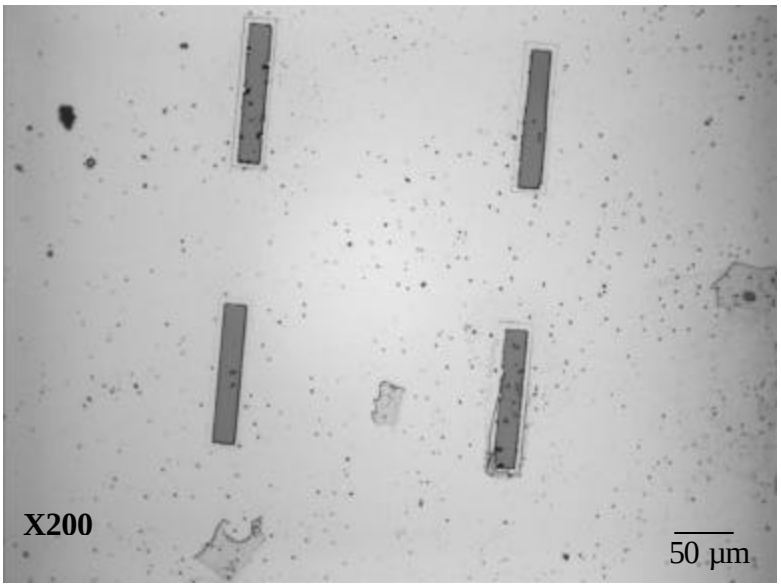

Figure 5.17: Microfabrication Pattern- Heavy Spots

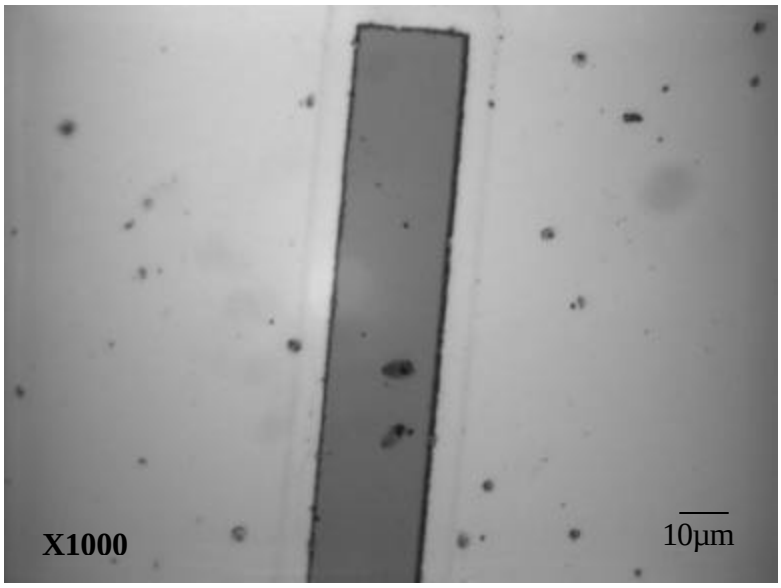

Figure 5.18: Microfabrication Pattern- Heavy Spots

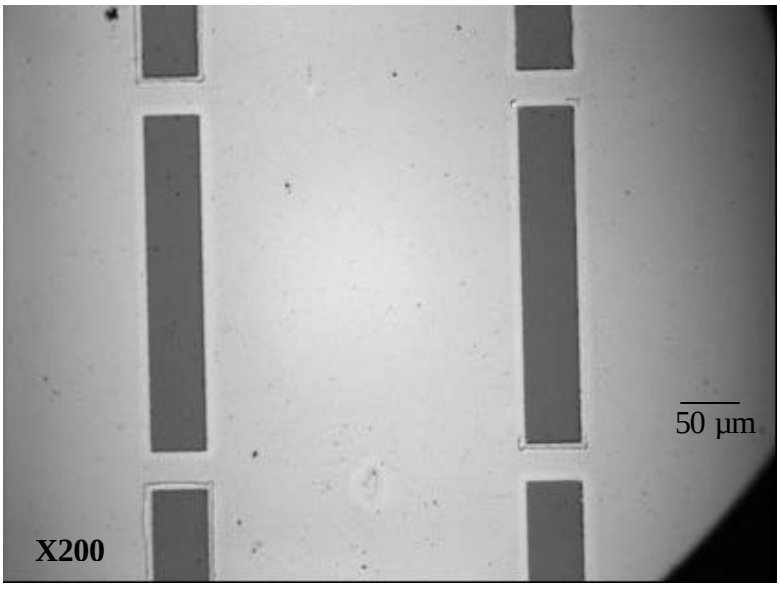

Figure 5.19: Microfabrication Pattern- Light Spots

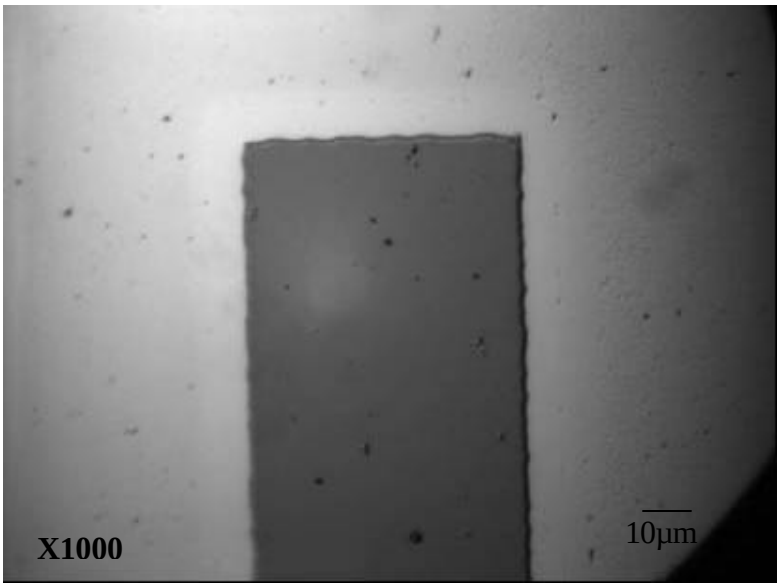

Figure 5.20: Microfabrication Pattern- Light Spots

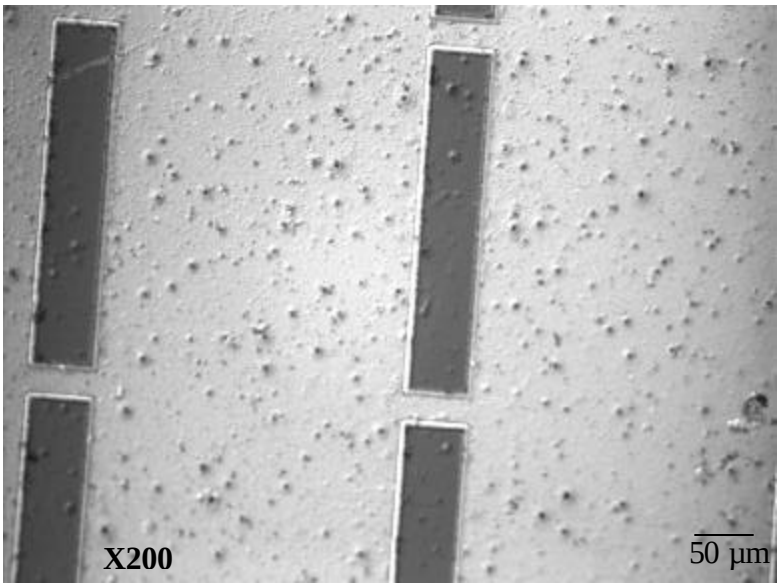

Figure 5.21: Microfabrication Pattern - Bubbles

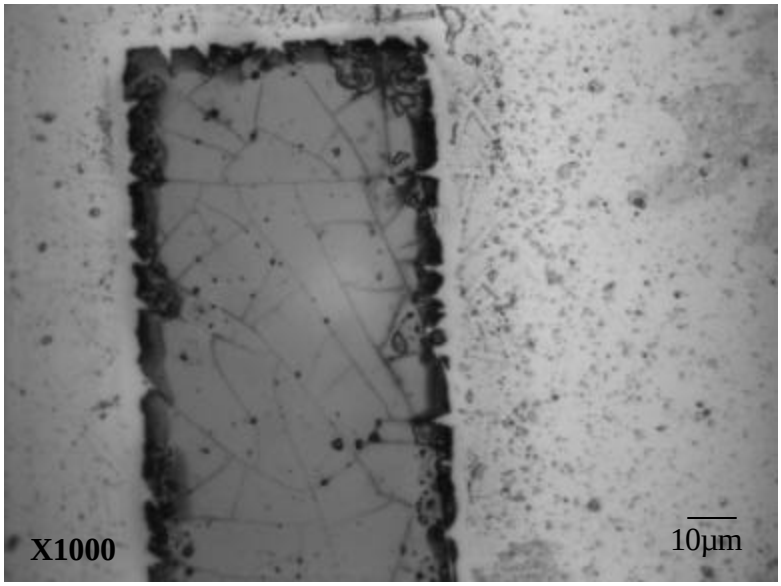

Figure 5.22: Microfabrication Pattern – Big Cracks

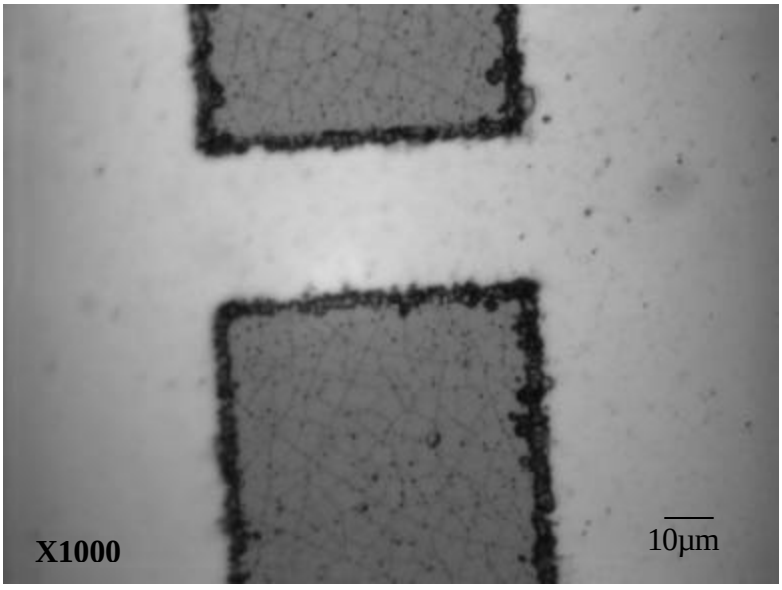

Figure 5.23: Microfabrication Pattern- Small Cracks

Figures 5.17-5.23 show the microfabrication pattern after the substrate has been etched. As can be seen from figure 5.17 through 5.20, the best results from patterning the sensor design on the thin film were the samples that contained only spots. Whenever a sample contained cracks in the thin film it was very noticeable after the samples were etched. The edges of the samples that contained cracks were very rugged (Figures 5.22 and 5.23). For the samples that contained bubbles the edges were fine, but the overall appearance of the sensors was questionable (Figures 5.21).

5.6: Conclusions

5.6.1: Magnetostrictive Microcantilever Biosensors:

As was stated in this thesis, magnetostrictive microcantilevers have many advantages over current microcantilevers. The principle advantage of magnetostrictive microcantilevers is that they can be driven and sensed wirelessly and that they have a high Q-value. They can be operated in a liquid media which is a crucial aspect for biosensing applications. The resonance frequency of magnetostrictive microcantilevers is directly related to the mass added on the sensor surface. The magnetostrictive microcantilevers researched in this thesis were used to detect different blood types. As can be seen in the results section, by observing shifts in resonance frequency due to blood cell loading there seems to be some potential in begin able to distinguish between certain blood types. In order to produce accurate consistent results issues related to reproducibility need to be performed in future work.

5.6.2: Magnetostrictive Thin Films:

A magnetostrictive material, iron boron, was successfully deposited on glass slides by electrochemical deposition. Different deposition combinations shown in the results section were used to try to eliminate the problems seen from deposition (such as spots, bubbles, cracks). The one problem that was consistent with all the deposition combinations was spots. Even after other variables were added this problem still arose. Overall the variables that seem to contain the best thin film were controlling the temperature of the deposition bath and the fresh solution. Controlling the temperature of the deposition bath will help reduce any internal stresses that may be taking place. Using a fresh solution to deposit the thin film will assure that no impurities are in the solution from a previous deposition sample. Since not enough samples were tested at a controlled temperature, it is not a fact that this indeed solved most of the problems seen earlier in deposition. The microfabrication of the magnetostrictive thin films was related to the deposition of the thin films. The best microfabrication results were seen when the deposition film contained only spots. Future work is still needed in order to determine the best deposition combination and to solve the problem of spots seen after deposition.

6. FUTURE WORK

Magnetostrictive Microcantilevers:

- Flow System
- Blocking Agent
- Cleaning Process

Future work for the magnetostrictive microcantilevers would include employing a flow system that would not allow samples to be touched multiple times by the user, and also to allow the cantilever to stay in one place. A blocking agent, for example immunopure biotinylated bovine serum albumin, on the surface of the sensor would increase the chances of non-specific binding. Improving the cleaning process of the cantilever needs to be studied so that this variable can be eliminated whenever negative results are produced.

Thin Film Project:

- Cleaning Process

In order to pinpoint which deposition parameter results in the best thin film, more experiments have to be completed. There were not enough samples tested at certain parameters to distinguish if that condition should be used or discarded. The main problem that was seen in the whole project was spots. Therefore different cleaning processes should be tested to see if the spots can be eliminated.

7. BIBLIOGRAPY

Andle, J. and Vetelino, J., "Acoustic wave biosensors," Sensors and Actuators A **44**, 167 (1994).

Battiston, F., Ramseyer, J., Lang, H., Baller, M., Gerber, C., Gimzewski, J., Meyer, E., and Guntherodt, H., "A chemical sensor based on a microfabricated cantilever array with simultaneous resonance-frequency and bending readout," Sensors and Actuators B **77**, 122 (2001).

Bokken, G., Corbee, R., Knapen, F., and Bergwerff, A., "Immunochemical detection of Salmonella group B, D, and E using an optical surface plasmon resoance biosensor," FEMS Microbiology Letters **222**, 75 (2003).

Campbell, C., "Applications of surface acoustic and shallow bulk acoustic wave devices," Proceedings of the IEEE **77,** 1453 (1989).

Cernosek, R., "Acoustic Sensors," Retrieved June 6, 2005, http://audfs.eng.auburn.edu/docs/bkgrnd-sensors.pdf.

Drafts, B., "Acoustic Wave Technology Sensors," IEEE Transactions on Microwave Theory and Techniques **49,** 795 (2001).

Eggins, B., Chemical Sensors and Biosensors, John Wiley and Sons Ltd Publishing. (2000).

Etienne du Tremolet de lacheisserie "Magnetostriction: Theory and Applications of Magnetoelasticity," CRC Press (1993).

Fagan, B., Tipple, C., Xue, Z., Sepaniak, M., and Datskos, P., "Modification of micro-cantilever sensors with sol-gels to enhance performance and immobilize chemically selective phases," Talanta **53,** 599 (2000).

Frankfurt, O. and Krishan, A., "Enzyme-linked immunosorbent assay (ELISA) for the specific detection of apoptotic cells andits applications to rapid drug screening," Journal of Immunological Methods **253**, 133 (2001).

Galipeau, D., Story, P., Vetelino, K., and Mileham, R., "Surface acoustic wave microsenosors and application," Journal of Smart Materials and Structures **6**, 658 (1997).

Ghindilia, A., Atanasov, P., Wilkins, M., and Wilkins, E., "Immunosensors: electrochemical sensing and other engineering approaches," Biosensors and Bioelectronics **13**, 113 (1998).

Giakoumaki, E., Minunni, M., Tombelli, S., Tothill, I., Mascini, M., Bogani, P., and Buiatti, M., "Combination of amplification and post-amplification strategies to improve optical DNA sensing," Biosensors and Bioelectronics **19**, 337 (2003).

Gizeli, E. and Lowe, C., "Immunosensors," Current Opinion in Biotechnology **7**, 66 (1996).

Grimes, C., Kouzoudis, D., Ong, K., and Crump, R., "Thin-film magnetoelastic microsensors for remote query biomedical monitoring," Biomedical Microdevices **2,** 51 (1995).

Hierlemann, A. and Baltes, H., "CMOS-based chemical microsensors," The Analyst **128**, 15 (2003).

Homola, J., Yee, S., and Gauglitz, G., "Surface plasmon resonance sesnsors:review," Sensors and Actuators B **54**, 3 (1999).

Ilic, B., Czaplewsli, D., Craighead, H., Neuzil, P., Campagnolo, C., and Batt, C., "Mechanical resonant immunospecific biological detector," Journal of Applied Physics Letters **77**, 450 (2000).

Ilic, B., Czaplewsli, D., Zalalutdinov, M., and Craighead, H., "Single cell detection with micromechanical oscillation," Journal of Vacuum Science and Technology **19**, 2858 (2001).

Ivnitski, D., Abdel-Hamid, I., Atanasov, P., and Wilkins, E., "Biosensors for detection of pathogenic bacteria," Biosensors and Bioelectronics **14**, 599(1999).

Kazuki, N. and Satsuo, K., "Rapid measurement of ABO blood typing by using SPR (surface plasmon resonance) sensor," Chemical Journal of Chinese Univeristies **20**, 499 (1999).

Kemeny, D. and Challacombe, S., "ELISA and Other Solid Phase Immounassays," Wiley, John & Sons, Incorporated. (1989).

Kim, Y., Flynn, T., Donoff, R., Wong, D. and Todd, R., "The Gene: The Polymerase Chain Reaction and Its Clincal Application," Journal of Oral Maxillofacial Surgery **60**, 808 (2002).

Koubova, V., Brynda, E., Karasova, L., Skvor, J., Homola, J., Dostalek, J., Tobiska, P., and Rosicky, J., "Detection of foodborne pathogens using surface plasmon resonance biosensors," Sensors and Actuators B **74**, 100 (2001).

Lang, H., Hegner, M., and Gerber, C., "Cantilever array sensors," Materials Today 8, 30 (2005).

Lee, H., Lee, H., Cho, M., and Lee, M., "Screening for penicillin residues in cattle by enzyme-linked immunosorbent assay," Acta Veterinaria Brno **70**, 353 (2001).

Luppa, P., Sokoll, L., and Chan, D., "Immunosensors- principles and applications to clinical chemistry," Clinica Chimica Acta **314**, 1 (2001).

Mehta, A., Cherian, S., Hedden, D., and Thundat, T., "Manipulation and controlled amplication of Brownian motion of microcantilever sensors," Journal of Applied Physics Letters **78**, 1637 (2001).

Mello, L. and Kubota, L., "Review of the use of biosensors as analytical tools in the food and drink industries," Food Chemistry **77**, 237 (2002).

Mertz, J., Marti, O., and Mlynek, J., "Regulation of a microcantilever response by force feedback," Journal of Applied Physics Letters **62**, 22344 (1993).

Myszka, D. and Rich, R., "Implementing surface plasmon resonance biosensors in drug discovery," Drug Discovery Today. 310 (2000).

Naimushin, A., Spinelli, C., Soelberg, S., Mann, T., Stevens, R., Chinowsky, T., Kauffman, P., Yee, S., and Furlong, C., "Airborne analyte detection with an aircraft-adapted surface plasmon resonance sensor system," Sensors and Actuators B **104**, 237 (2005).

Nunes, G., Toscano, I., and Barcelo, D., "Analysis of pesticides in food and environmental samples by enzyme-linked immunosorbent assays," Trends in Analytical Chemistry **17**, 79 (1998).

Piletsky, S., Piletska, E., Bossi, A., Karim, K., Lowe, P., and Turner, A., “Substitution of antibodies and receptors with molecularly imprinted polymers in enzyme-linked and fluorescent assays,"Biosensors and Bioelectronics **16**, 701 (2001).

Puckett, L., Barrett, G., Kouzoudis, D., Grimes, C., and Bachas, L., "Monitoring blood coagulation with magnetoelastic sensors," Biosensors and Bioelectronics **18**, 675 (2003).
Qing, Y. and Grimes, C., "A remote query magnetoelastic pH sensor," Sensors and Actuators B **71**, 112 (2000).

Qing, Y., Mahaveer, K., and Grimes, C., "A wireless, remote query ammonia sensor," Sensors and Actuators B **77**, 614 (2001).

Raiteri, R., Grattarola, M., and Berger, R., "Micromechanics senses biomolecules," Materials Today 5, 22 (2002).

Raiteri, R., Grattarola, M., Butt, H., and Skladal, P., "Micromechanical cantilever-based biosensor," Sensors and Actuators B **79**, 115 (2001).

Read, D., "Young's modulus of thin films by speckle interferometry," Measurmennt Science and Technology 9, 676 (1998).

Ruan, C., Zeng, K., and Grimes, C., "A mass-sensitive pH sensor based on a stimuli-responsive polymer," Analytica Chimica Acta **497**, 123 (2003).

Shen, Y., Shen, C., and Wu, L., "Design of ST-cut quartz surface acoustic wave chemical sensors," Sensors and Actuators B **85**, 277 (2002).

Shiokawa, S. and Kondoh, J., "Surface Acoustic Wave Sensors," Japanese Journal of Applied Physics **43**, 2799 (2004).

Tamayo, J., Humphris, A., Malloy, A., and Miles, M., "Chemical sensors and biosensors in liquid environment based on microcantilevers with amplified quality factor," Ultramicroscopy **86**, 167 (2001).

Ul-Hassan, S., Verma, V., and Qazi, G., "Rapid detection of salmonella by polymerase chain reaction," Molecular and Cellular Probes **18**, 333 (2004).

Van, R., "Applications of the Polymerase Chain Reaction to Diagnosis of Ophthalmic Disease," Survey of Ophthalmology **45**, 248 (2001).

Watanabe, K., Doi, Y., Shigeta, Y., Suzuki, S., and Katsu, T., "Highly sensitive method for determination of ABO blood groups using absorption-elution test combined with ELISA and its automation," Japanese Journal of Science and Technology for Identification **7**, 71 (2002).

Weinberg, M., Cunningham, B., and Clapp, C., "Modeling flexural plate wave devices," Journal of Microelectro-Mechanical Systems **9**, 370 (2000).

.

Wenzel, S. and White, R., "Flexural plate-wave gravimetric chemical sensor," Sensors and Actuators A **22**, 700 (1990).

Yang, M., Zhang, X., Vafai, K., and Ozkan, C., "High sensitivity piezoresisitive cantilever design and optimization for analyte-receptor binding," Journal of Micromechanics and Microengineering **13**, 864 (2003).

Yi, J., Shih, W., Mutharasan, R., and Shih, W., "In situ cell detection using piezoelectric lead zirconate titanate-stainless steel cantilevers," Journal of Applied Physics **91**, 619 (2003).

Yi, J., Shih, W., and Shih, W., "Effect of length, width, and mode on the mass detection sensitivity of piezoelectric unimorph cantilevers," Journal of Applied Physics **93**, 619 (2003).

Zhou, J., Li, P., Zhang, S., Huang, Y., Yang, P., Bao, M., and Raun, G., "Self-excited piezoelectric microcantilever for gas detection," Microelectronic Engineering **69**, 37 (2003).

Ziegler, C., "Cantilever based-biosensors," Anal Bioanal Chem. **379**, 946 (2004).

…Biacore, "Surface Plasmon Resonance (SPR)," Retrieved June 6, 2005, http://www.cancer.bham.ac.uk/staff/benjaminw/web/spr.html.

…Biology II Anatomy and Physiology, "Blood Types," Retrieved June 6, 2005, http://www.sirinet.net/~jgjohnso/circulation.html.

…Crestwood Medical Center, "Blood banking," Retrieved June 6, 2005, http://www.crestwoodmedcenter.com/CustomPage.asp?PageName=Lab%20-%20Bloodbanking.

…Dr. Joseph F. Smith Medical Library, "Blood typing and cross matching," Retrieved April 25, 2005, www.chclibrary.org/micromed/00040190.html.

…Ferromagnetism, "Magnetic Domains," Retrieved June 6, 2005, http://hyperphysics.phy-astr.gsu.edu/hbase/solids/ferro.html#c1.

…Franklin Institute Online, "What's your type?" Retrieved April 24, 2005, http://sln.fi.edu/biosci/blood/types.html.

…Genetic Science Learning Center at the Univeristy of Utah, "What are blood types?" Retrieved April 25, 2005, http://gslc.genetics.utah.edu/units/basics/blood/types.cfm.

…Iowa State University:Welcome to Magnetostrictive Transducers, Actuators, and Sensors , "What is a Magnetostrictive," Retrieved June 6, 2005, http://www.public.iastate.edu/~terfenol/homepage.html.

…LABMEDICNE, "Evaluation of an automated system for ABO/D typing and RBC antibody detection system in a hospital transfusion service," Retrieved June 6, 2005, http://www.labmedicine.com/2005/Issue-01/1001002.html.

…MSN Encarta, "Polymerase Chain Reaction," Retrieved June 6, 2005, http://encarta.msn.com/media.

…Univeristy of Waterloo, Physics department, "Surface Plasmon Resonance," Retrieved April 25, 2005, http://www.lorenz-steinbock.de/plasmon.pdf.